

NISTIR 6400

Development of an Apparatus for Measuring the Thermal Performance of Fire Fighters' Protective Clothing

J. Randall Lawson
William H. Twilley



U.S. Department of Commerce
Technology Administration
National Institute of Standards and Technology
Gaithersburg, MD 20899



Sponsored in part by:
Federal Emergency Management Agency
U.S. Fire Administration
Emmitsburg, MD 21727-8998

Development of an Apparatus for Measuring the Thermal Performance of Fire Fighters' Protective Clothing

J. Randall Lawson
William H. Twilley

October 1999



U.S. Department of Commerce
William M. Daley, *Secretary*
Technology Administration
Gary R. Bachula, *Under Secretary for Technology*
National Institute of Standards and Technology
Raymond G. Kammer, *Director*



Sponsored in part by:
Federal Emergency Management Agency
James Lee Witt, *Director*
U.S. Fire Administration
Carrye B. Brown, *Administrator*

TABLE OF CONTENTS

LIST OF FIGURES	iv
Abstract	1
1.0 INTRODUCTION	2
2.0 OBJECTIVE	3
3.0 TEST APPARATUS AND MEASUREMENT PROCEDURES	3
3.1 GENERAL DESCRIPTION	3
3.2 TEST APPARATUS	4
3.2.1 HEAT AND FLAME EXPOSURE APPARATUS	4
3.3 APPARATUS INSTRUMENTATION AND DATA ACQUISITION	5
3.3.2 BASIC TEST INSTRUMENTATION	5
3.3.3 OTHER INSTRUMENTATION CONFIGURATIONS	7
3.3.4 DATA ACQUISITION	7
3.4 TEST PROCEDURE	7
3.4.1 TEST SPECIMEN CONDITIONING	7
3.4.2 RADIANT HEAT SOURCE CALIBRATION	7
3.4.3 PILOT FLAME ADJUSTMENT AND COMBINED HEAT FLUX CALIBRATION	8
3.4.4 PRACTICE USED FOR CONDUCTING TESTS	8
3.5 METHOD FOR WETTING TEST SPECIMENS	9
4.0 TEST PRECISION	9
5.0 TEST DESCRIPTIONS AND RESULTS	11
5.1 1.0 kW/m ² HEAT FLUX TESTS	12
5.2 2.5 kW/m ² HEAT FLUX TESTS	12
5.3 RADIANT HEAT FLUX TESTS WITH FLAMES	13
5.4 OPEN AND CLOSED BACK SPECIMEN TESTS	14
6.0 SUMMARY	16
7.0 FUTURE RESEARCH	16
8.0 ACKNOWLEDGMENTS	17
9.0 REFERENCES	18

LIST OF FIGURES

Figure 1	Photograph of test apparatus	20
Figure 2	Sketch, side view of test apparatus	21
Figure 3	Sketch, front view of test apparatus	22
Figure 4	Sketch of trolley assembly	23
Figure 5	Sketch of thermal radiation shield	24
Figure 6	Sketch of pilot burner assembly	25
Figure 7	Sketch of calibration board and specimen holder	26
Figure 8	Sketch of open back and closed back specimen holders	27
Figure 9	Sketch showing stitching for thermocouple attachment	28
Figure 10	Recommended thermocouple locations used for standard testing.	29
Figure 11	Thermocouple locations used for data shown in figures 18 through 22	30
Figure 12	Additional thermocouple locations used for flaming exposures in figures 23a, 23b, and 23c.	31
Figure 13	Thermocouple locations used with open and closed back tests	32
Figure 14	Variation of front surface thermocouple measurements for eight tests.	33
Figure 15	Variation of back surface thermocouple measurements for eight tests.	34
Figure 16	Variation of mid-point thermocouple measurements for eight tests.	35
Figure 17	Data plots for thermocouple radiant heat flux error test.	36
Figure 18	Data plots from 1.0 kW/m ² heat flux test	37
Figure 19	Data plots from 2.5 kW/m ² heat flux test with dry thermal liner.	38
Figure 20	Data plots from 2.5 kW/m ² heat flux test with 38 grams of water on thermal liner	39
Figure 21	Data plots from 2.5 kW/m ² heat flux test with 25 grams of water on thermal liner	40
Figure 22	Data plots from dry specimen test, 1.0 kW/m ² radiant plus flame ~ 35 kW/m ²	41
Figure 23a	Data plots from 2.5 kW/m ² , 20 kW/m ² , plus flame test, dry specimen, top thermocouple set.	42
Figure 23b	Data plots from 2.5 kW/m ² , 20 kW/m ² , plus flame test, dry specimen, center thermocouple set.	43
Figure 23c	Data plots from 2.5 kW/m ² , 20 kW/m ² , plus flame test, dry specimen, bottom thermocouple set.	44
Figure 24	Data plots for a dry, open back, nonbreathable specimen at 2.5 kW/m ²	45
Figure 25	Data plots for a dry, closed back, nonbreathable specimen at 2.5 kW/m ²	46
Figure 26	Data plots for a dry, open back, breathable specimen	47
Figure 27	Data plots for a dry, closed back, breathable specimen at 2.5 kW/m ²	48
Figure 28	Data plots for wet, open back, nonbreathable specimen at 2.5 kW/m ²	49
Figure 29	Data plots for a wet, closed back, nonbreathable specimen at 2.5 kW/m ²	50
Figure 30	Data plots for a wet, open back, breathable specimen at 2.5 kW/m ²	51
Figure 31	Data plots for a wet, closed back, breathable specimen at 2.5 kW/m ²	52

DEVELOPMENT OF AN APPARATUS FOR MEASURING THE THERMAL PERFORMANCE OF FIRE FIGHTERS' PROTECTIVE CLOTHING

by

J. Randall Lawson and William H. Twilley

Abstract

Fire fighters' protective clothing has steadily improved over the years as new materials and improved designs have reached the market. A significant catalyst that has brought these improvements to the fire service is the National Fire Protection Association (NFPA) 1971 standard on structural fire fighters' protective clothing. The fabric flammability test in this standard has resulted in the development of protective garments that resist flaming ignition. The Thermal Protective Performance (TPP) test has assisted in the development of garments that protect fire fighters from short duration, high intensity, flash fire exposures. These two thermal tests methods have clearly lead to improvements in fire fighter safety. However, thousands of fire fighters are continuing to be seriously burned each year. Discussions with fire service personnel indicate that many of these serious burn injuries are occurring when fire fighters are exposed to thermal environments that are significantly less intense than those addressed in the NFPA standard. Therefore, the National Institute of Standards and Technology (NIST) has begun the development of a method for measuring the thermal performance of fire fighters' protective clothing under thermal conditions less severe than those currently specified in NFPA 1971.

This report describes a test apparatus and investigates a method for measuring the thermal performance of fire fighters' protective clothing. The test method measures temperature through the various layers that make up a fire fighter's thermal protective garment. Temperature measurements are made at the surface of the outer shell, at locations between fabric or moisture barrier layers inside the protective clothing system, and at the thermal liner surface where the fire fighter's clothing or body would be in contact with the garment. When plotted, these temperature measurements show a detailed picture of how a protective clothing system performs when exposed to a given thermal environment. The apparatus may be used to expose protective clothing specimens to a wide range of heat flux conditions. These thermal conditions may be varied from 1.5 kW/m^2 to more than 50 kW/m^2 . The test apparatus may be used for investigating the effects of moisture in protective clothing systems. In addition, this test apparatus and the measurement methods allow for specimens to be studied for a time period ranging from several seconds to more than 30 minutes.

KEY WORDS: Environments, fires, fire fighters, heat transfer, burns (injuries), protective clothing, test method

1.0 INTRODUCTION

Fire fighters' protective clothing has been designed to provide the wearer with a limited amount of protection from burn injury if suddenly exposed to an intense short duration flash fire or short time exposure to a flashover condition. This level of protection has been made possible through the development of new heat resistant fabrics, insulating materials, and the use of NFPA1971[1]. This standard specifies test methods that quantify thermal performance of protective clothing. Two thermal performance test methods found in NFPA 1971 have had a significant impact on the performance of fire fighters' protective clothing. The fabric flammability test has resulted in the development of protective garments that resist flaming ignition. The Thermal Protective Performance (TPP) test has helped in the design of protective garments that reduced the rate of heat flow from a fire fighting environment through the protective clothing.

The TPP test measures heat flow through the garment while exposed to a 84 kW/m^2 ($2 \text{ cal/cm}^2\cdot\text{s}$) thermal environment that is intended to simulate a flash fire or mid-range post-flashover exposure. A single copper calorimeter is used to measure heat transfer through a protective clothing assembly, and no data is gathered on the thermal performance of individual protective clothing components. The NFPA standard specifies a minimum TPP rating of 35. Work by Krasney et al., suggests that fire fighters wearing TPP 35 garments will likely receive serious burn injuries in less than 10 seconds when exposed to a flashover fire environment [2]. Fortunately, very few fire fighters are enveloped by flashover conditions while fire fighting. Most fire fighter burn injuries appear to result from thermal exposures much less severe than the post-flashover conditions used by the TPP test. In addition, many burn injuries appear to result from relatively long duration low to moderate heat flux exposures. TPP test measurements are time restricted based on the thermal properties of the copper calorimeter. Therefore, TPP tests on thermal protective clothing have been conducted using time periods generally less than one minute [1].

Many fire fighter burn injuries occur from exposures to radiant heat energy that is produced by a fire. In other cases, fire fighters are burned by a combination of radiant energy and localized flame contact exposures. Some injuries occur as a result of compressing the protective garment against the skin, either by touching a hot object or by placing tension on the garment fabric until it becomes compressed against the skin. In addition to these mechanisms, moisture in protective clothing can significantly change the garment's protective performance. As stated in NISTIR 5804, garments that are wet may exhibit significantly higher heat transfer rates than garments that are dry [3]. Burn injuries that result from the heating and evaporation of moisture trapped within one's protective clothing is also significant. These injuries are generally referred to as scald or steam burns. Moisture may also help to store heat energy in protective clothing [3].

There are many unanswered questions about the affects of heat energy that is stored in fire fighters' protective clothing. This heat energy may be accumulated in protective clothing during relatively short exposures to a fire fighting environment or over an extended time period. NFPA 1971 does not currently require tests for measuring heat energy that can be stored in fire fighters' protective clothing. The NFPA 1971 Technical Committee has attempted to use the TPP test apparatus for

measuring stored heat energy in fire fighter's protective clothing. These efforts have not been totally successful, especially when trying to make measurements on wet garment systems. Upon considering all of the conditions discussed above that may cause serious burn injuries, a new test apparatus and measurement techniques are being developed that will provide fresh insight into the thermal performance of fire fighters' protective clothing. This test apparatus may be used to measure the thermal performance of fire fighters' protective clothing over a wide range of environmental conditions and over extended time periods. In addition to describing the apparatus and a proposed approach to testing, this report presents examples of thermal performance test data for fire fighters' protective clothing systems with surface attachments fastened to the garment's shell fabric.

2.0 OBJECTIVE

The objectives of this study are as follows: a) Design an apparatus capable of exposing specimens of fire fighters' protective clothing to a wide range of controlled and reproducible heat flux conditions, b) Develop an approach for measuring the thermal response of individual components of a protective clothing system while they are a part of the composite assembly, and c) Identify needs and provide recommendations for future research on measuring the thermal performance of fire fighters' protective clothing.

3.0 TEST APPARATUS AND MEASUREMENT PROCEDURES

3.1 GENERAL DESCRIPTION

The test apparatus allows for evaluating the thermal performance of protective clothing systems exposed to heat flux environments ranging from about 1.5 kW/m^2 to more than 50 kW/m^2 . A pilot flame may be placed onto the test specimen during any part of a test to evaluate thermal performance associated with direct flame contact. Protective clothing specimens may also be tested wet so that the effects of moisture can be studied. Measurement data obtained using this test apparatus provide time/temperature response histories for components of protective clothing assemblies. Thermocouples may be used for measuring temperatures at any location of interest on or inside the test specimen assembly. In addition, measurement methods may be used for determining the latent heat or amount of energy stored in the garment assembly upon being exposed to a selected thermal environment for a specified period of time. The amount of heat energy stored in a protective garment system may be estimated using mathematical techniques similar to those discussed in NISTIR 6299 [4]. The report by Mell and Lawson provides information on a computer based method for quantifying heat energy in a protective clothing system. Data from this computer based method may be useful in predicting protective clothing system thermal exposure times that relate to potential burn injury.

Section 3.2 provides a detailed description of the test apparatus described in this report, and section 3.3 describes test apparatus instrumentation.

3.2 TEST APPARATUS

3.2.1 HEAT AND FLAME EXPOSURE APPARATUS

The test apparatus and its components are shown in figures 1 through 6. Radiant heat energy for this test is produced by a premixed air/natural gas fueled radiant panel with a radiating surface measuring 305 mm by 457 mm (12 in by 18 in). The radiant panel type is specified in ASTM E162, Standard Test Method for Surface Flammability of Materials Using a Radiant Heat Energy Source [5]. This radiant panel is normally operated at an average surface blackbody temperature of $670 \pm 4^{\circ}\text{C}$ ($1238 \pm 7^{\circ}\text{F}$). A propane gas pilot line burner allows for applying a flame directly across the test specimen's width. See figures 1, 2, and 6 for the burner's location on the test apparatus and construction details. The flame height may be adjusted to a low level for determining if fabrics or surface finishes will ignite or the height may be increased to sweep across a specimen's complete surface. The pilot burner is constructed so that it may be rotated toward or away from the test specimen's front surface. The pilot burner may be fixed in place or it may be moved along the trolley rail to any location required for a specified test scenario.

3.2.2 TEST SPECIMENS

Test specimens, figures 7 and 8, measure 305 mm x 305 mm (12 in x 12 in) square. The specimen's surface exposed to test conditions, when held in the specimen holder, measures 255 mm x 255 mm (10 in x 10 in). See photograph showing the test specimen prepared for test in figure 1 and the sketch of the specimen holders in figure 8. This specimen size was selected to allow for testing of protective clothing system designs that have surface features (i.e., trim, pads, patches, or pockets) that may require evaluation. Test specimens described in this report were made with four components as layered from the garment's outside surface: 1) reflective trim, 2) shell fabric, 3) moisture barrier, and 4) thermal liner. The reflective trim material was machine sewed to the shell fabric layer, as it would be attached to a garment, with the trim centerline positioned along the vertical centerline of the specimen. The selection of this test specimen assembly allows for making comparative measurements of thermal response for reflective trim covered areas on a protective garment to the thermal response of areas that did not have trim attached. This specimen configuration represents the construction of a typical thermal protective garment used by the fire service.

Two different types of test specimen holders are used. The holders are shown in figures 7 and 8. One specimen holder uses a completely open frame that allows the front and back specimen surfaces to be observed during a test. The other specimen holder has a closure on its back side. The closure system has a 6.4 mm (0.25 in) aluminum spacer placed between the test specimen's back surface (garment layer that would be closest to the human body) and the solid closure assembly. The spacer provides a small air gap in an attempt to replicate the space between a fire fighter's protective clothing and their work uniform. This solid closure assembly is constructed of 12 mm (0.5 in) thick calcium silicate board covered on one side with a 1.6 mm (0.063 in) thick phenolic sheet. The entire assembly is covered with a smooth layer of 100% cotton knit "T" shirt material.

Tests may be conducted with either an open back or closed back configuration. Section 5.4 discusses test results that compare open back and closed back test configurations. The open back configuration allows the test operator to observe both sides of the test specimen for physical changes. The closed back configuration reduces heat loss from the back side by replacing the open back portion of the specimen holder with a closure. It is estimated that the actual thermal performance of fire fighters' protective clothing exists at some condition between the open back and closed back configuration. The open back configuration provides for unrestricted heat loss, and the closed back configuration reduces heat loss from the specimen's back side. Even though fire fighter's protective clothing is considered to be a closed system in use, it does not duplicate the static closed back configuration used in this test. In actual field use, garment ventilation and heat loss is affected by variations in garment fit, ease or space between the garment and the wearer, and air movement in a garment resulting from pumping actions caused by body movements. A sketch of the open and closed back test specimen holders are shown in figure 8.

Test specimens are mounted on the movable trolley assembly that is attached to the radiant panel test frame. Positioning of the trolley allows for adjustment of radiant flux exposures and provides the ability to expose test specimens to radiant energy environments that can be increased or decreased during a test. Solar heat flux level exposures, approximately 1.0 kW/m^2 , are obtained by reducing the radiant panel's gas flow which reduces the radiant panel's surface temperature. In addition, the test specimen trolley is moved to the most distant location from the radiant panel.

3.3 APPARATUS INSTRUMENTATION AND DATA ACQUISITION

3.3.1 CALIBRATION

A calibrated Schmidt-Boelter total heat flux transducer of the type specified in ASTM E1321, Standard Test Method for Determining Material Ignition and Flame Spread Properties [6] is used for measuring heat flux levels. This water cooled, thermopile type, heat flux transducer has a nominal range of 0 kW/m^2 to 50 kW/m^2 with a sensitivity of approximately 10 mV at 50 kW/m^2 . The time constant for this heat flux gauge is not more than 290 ms with a corresponding time to reach 95% of the final output of not more than 1 s . The heat flux gauge measures 25 mm (1 in) in diameter and has a metal flange located 25 mm (1 in) down its body, away from the sensing surface.

3.3.2 BASIC TEST INSTRUMENTATION

Type K thermocouples with a wire diameter of 0.254 mm (0.010 in) are used to obtain temperature data. Thermocouple attachment is shown in figure 9, and the basic thermocouple locations are shown in figure 10. A minimum of three thermocouples are required for making heat flow measurements through a garment assembly. These are thermocouples 1, 2, and 3 shown in figure 10. Thermocouple number 4 may be used to measure open field temperatures when a surface attachment is applied to the shell material. The three basic thermocouples are also needed for measuring the amount of heat energy stored in protective clothing systems.

Thermocouples are prepared and attached using the following procedures. Thermocouple wires that form the bead or junction are stripped of insulation for a minimum of 10 mm (0.39 in) and not more than 20 mm (0.78 in) from the bead. Thermocouple attachment is shown in figure 9. These thermocouples are sewed directly to the surface of the test specimen fabrics using cotton or flame resistant thread having a maximum diameter of 0.254 mm (0.010 in). Care must be taken to keep the thermocouple beads and bare wires in direct contact with the fabric's surface without having the thread come between the thermocouple bead and the test fabric. Also, efforts are made to keep the thermocouple leads from being located over any needle holes caused by sewing. For strain relief near the specimen's edge, high temperature glass fiber electrical tape may be substituted for thread stitching. The use of tape for strain relief will reduce the time require for specimen preparation. Tape is not recommended for use to hold the thermocouple beads to the fabric. Thermocouple performance may be altered if tape is placed directly on stripped wires near or over the thermocouple junction. Basic thermocouple locations are shown in figure 10. Three or four thermocouples are used in the basic test configuration. They are attached at the following locations: One thermocouple is sewed to the outer shell fabric at the specimen's center. If trim or another surface attachment is being tested as a part of the protective clothing specimen, this thermocouple is attached at the vertical center and horizontally displaced from the trim's edge by 10 mm (0.39 in) and is sewed to the shell fabric. Either of these thermocouples may be referred to as the **front surface (1)** thermocouple. The second thermocouple is sewed to the inside surface of the thermal liner fabric that is located between protective clothing layers. This thermocouple is referred to as the **mid-point (2)** thermocouple. The thermocouple is attached along the vertical centerline and 10 mm below the front surface thermocouple position. The third thermocouple is sewed to the fabric that is located next to what would be the human body. This thermocouple is identified as the **back surface (3)** thermocouple. This thermocouple is located near the vertical and horizontal center lines behind the front surface thermocouple, but it is offset above the front surface thermocouple by 10 mm (0.39 in). The 10 mm (0.39 in) offset on the mid-point and back surface thermocouples prevents shading of heat energy from the other thermocouple wires attached to the test specimen. If trim or other surface attachments are secured to the shell fabric, the back surface thermocouple is attached at the specimen's center directly behind the specimen's centerline. Also, if trim or other surface attachments are used on the shell fabric, a fourth thermocouple is added to allow for the comparison of heat flow through the attachment covered area and the specimen area not covered by the surface attachment. This thermocouple is sewed to the fabric that would be located closest to the human body or work uniform. The thermocouple is located on the same vertical plane as the front surface thermocouple, but it is located 10 mm (0.39 in) below the front surface thermocouple. This extra thermocouple is identified as the **back surface, beside attachment (4)** thermocouple.

Notes of caution: All thermocouple wires must be located and run across the test specimen so that they do not interfere with the other thermocouples or components of the test specimen. Strain relief stitches must be placed around each thermocouple wire near the specimen's edge as shown in figure 9. High temperature tape may be substituted for strain relief at the same location. Strain relief is provided to help keep the thermocouples in place while the specimen is being put in the test frame and to reduce the chances of sensor movement during the test. In addition, it has been noted that quilted thermal barrier fabric systems with thermocouples sewed near the compressed areas where

quilt stitching is located generally tend to register higher temperatures than thermocouples sewed to quilt areas with normal loft.

3.3.3 OTHER INSTRUMENTATION CONFIGURATIONS

Figure 11 exhibits thermocouple locations for test data shown in figures 18 through 22. See sections 5.1 and 5.2. Figure 12 shows the placement of additional thermocouples used for collecting data shown in figures 23a, 23b, and 23c. The experimental results shown in figures 23a, 23b, and 23c used a pilot flame in conjunction with radiant heat energy from the gas fired radiant panel. The thermocouple pattern, figure 12, in this experiment was developed to better define temperature conditions across the test specimen when the flaming pilot is applied. A discussion of this experiment is found in section 5.3. Figure 13 illustrates the placement of additional specimen thermocouples used during the evaluation of open and closed back testing. This thermocouple configuration was used to better define the thermal performance of individual garment system components. This (open back/closed back) specimen holder study is discussed in section 5.4. All of the thermocouples discussed in this section were attached with the same materials and procedures as given above for the other thermocouples.

3.3.4 DATA ACQUISITION

A computer controlled data logger was used for recording results reported in this paper. The data logger had eight input channels, and data were recorded from each channel, that was used, every second. The data logger contained a cold junction temperature compensation device for correcting test thermocouple measurements to a reference junction temperature of 0°C (32°F).

3.4 TEST PROCEDURE

Tests reported in this work were conducted using the following general procedure. The procedure was modified slightly for evaluations where moisture was added to the garment materials.

3.4.1 TEST SPECIMEN CONDITIONING

Test specimens were conditioned in a controlled laboratory environment. This environment was $23^{\circ}\text{C} \pm 3^{\circ}\text{C}$ ($70^{\circ}\text{F} \pm 5^{\circ}\text{F}$) $50\% \pm 10\%$ relative humidity. Test room conditions with the radiant panel operating was typically $28^{\circ}\text{C} \pm 2^{\circ}\text{C}$ ($82^{\circ}\text{F} \pm 4^{\circ}\text{F}$).

3.4.2 RADIANT HEAT SOURCE CALIBRATION

First, the thermal environment was selected for a series of tests. The gas fired radiant panel was ignited and allowed to preheat for 45 minutes. This preheat time allowed the radiant panel's temperature to stabilize before calibration was attempted. Using the calibration coefficient for the Schmidt-Boelter heat flux gauge, the millivolt output value was calculated for the selected incident heat flux. An inorganic calcium silicate calibration board with a hole located at its geometric center

was attached to the trolley's specimen holder frame, figure 7. The heat flux gauge hole was cut slightly larger than the heat flux gauge diameter so that the gauge could easily be inserted into the board and held in place. The calibrated heat flux gauge, as described in section 3.1, was attached to a calibrated digital millivolt meter and was placed into the calibration board hole. The thermal radiation screen was kept in place until ready to calibrate. Heat flux gauge cooling water was turned on, and the flow rate was adjusted to $0.57 \text{ l/min} \pm 0.2 \text{ l/min}$ ($0.15 \text{ gal/min} \pm 0.05 \text{ gal/min}$). The thermal radiation screen (figures 2 and 5) was removed, and the gauge was allowed to heat until the signal output became relatively stable. This usually took only a few seconds. The specimen trolley (figure 2 and 4) was either moved toward or away from the radiant panel to determine the location that produced the desired heat flux. The test location was marked and recorded with the millivolt output and heat flux value. Rail locks were put into place to keep the test specimen trolley from moving. When two or more heat flux exposure conditions were needed for an experiment, the trolley was moved to positions that produced the desired heat flux, and the above marking procedure was repeated. A trolley rail lock was placed on the rail at the closest and most distant marked locations from the radiant panel.

3.4.3 PILOT FLAME ADJUSTMENT AND COMBINED HEAT FLUX CALIBRATION

When the pilot flame was used (figures 2 and 6), its specimen contact position was established before the test. Also, flame height was adjusted and quantified to account for the additional heat flux developed by the pilot flame. This calibration was done with the radiant panel operating and after the above calibration was completed.

3.4.3.1 With the specimen trolley located at the desired test position, as determined by section 3.4.2, the pilot flame assembly was moved to the desired location on the calibration board. The pilot burner was ignited and flame was adjusted to the desired height.

3.4.3.2 Combined heat flux from the radiant panel and pilot flame was measured by placing the water cooled total heat flux gauge into the calibration board and then following the procedure described in section 3.4.2

3.4.4 PRACTICE USED FOR CONDUCTING TESTS

3.4.4.1 After calibrating the apparatus, a thermal radiation screen was placed between the radiant panel and the trolley specimen frame.

3.4.4.2 A preconditioned specimen with thermocouples already attached was placed in the specimen holder, and the holder was bolted together. Figures 7 and 8 show holder assembly.

3.4.4.3 The specimen holder with the specimen mounted in it was secured to the specimen frame. A loose reflective cover made from aluminum foil was placed over the test specimen's front surface to shade it from reflected heat energy. This reflective cover was suspended so it was not less than 50 mm (2 in) from the specimen's front surface.

3.4.4.4 The thermocouple wires were plugged into the data logger.

3.4.4.5 The data logger was started and was allowed to run for a minimum of 15 seconds to develop a test baseline.

3.4.4.6 When the baseline was established, the thermal radiation screen and aluminum foil were quickly removed, starting the test.

3.4.4.7 The thermal exposure continued. When multiple exposure times and thermal flux levels were desired, the specimen trolley was moved at the selected times to precalibrated marked locations to obtain the next exposure. When the test used a flaming exposure, the pilot flame was ignited and placed onto the specimens front surface at the time selected.

3.4.4.8 The thermal exposure was ended by quickly moving the specimen trolley to the most distant location from the radiant panel and placing the thermal radiation screen between the radiant panel and the test specimen. The aluminum foil reflective cover was quickly placed over the specimen's front surface being sure to maintain a 50 mm (2 in) clearance.

3.4.4.9 Data logging was stopped at the test's end, and the data were saved for analysis and reporting.

3.5 METHOD FOR WETTING TEST SPECIMENS

Because fire fighters' protective clothing is designed to help keep the wearer dry, wetting of test specimens may be difficult. This is particularly the case where fabrics are new, they have been treated with water repelling chemicals, and/or they have not been soiled or pre-washed. Fabric properties and garment construction often make it difficult to evenly add moisture to fire fighters' protective clothing. A non-uniform application of moisture to a protective clothing system may cause significant variations in test results. The following wetting procedure proved adequate for the wet specimen tests shown in this report. However, more detailed procedures may be required for other types of materials used in the fabrication of fire fighters' protective clothing.

Wet test specimens were prepared by laying the specimen out flat on a laboratory bench and spraying distilled water onto its surface with a laboratory spray bottle. A mask was placed over the test specimen's surface that allowed water to only be sprayed onto a specimen area measuring 254 mm x 254 mm (10 in x 10 in) square. A spray bottle was filled with distilled water, and then it was placed onto a calibrated electronic laboratory balance. The bottle and water weight was recorded. Water was then evenly sprayed onto the protective clothing fabric, and the spray bottle was weighed again to determine the amount of water distributed onto the test specimen. This process was continued until the desired amount of water was sprayed onto the specimen. In some cases water would not adhere to the specimen's surface. In these cases, water that was sprayed onto the fabric was rubbed into the fabric by using finger tips or light strokes of a tooth brush. Depending on the test, water was applied to the shell fabric's surface; between the shell material and the moisture barrier by spraying water onto the inside of the shell fabric or onto the moisture barrier's surface; and water was sprayed onto the woven fabric side of the thermal barrier.

4.0 TEST PRECISION

With the basic dry test, there are five variables that relate to precision: 1) variation in thermocouple attachment, 2) variation in heat flux, 3) data logger resolution for voltage measurement, 4) thermocouple response time, and 5) data logger sample rate precision. The variation in

thermocouple attachment, item 1, ranged over a 10 °C (18 °F) change for all uncertainty. Heat flux variation to the test specimen, item 2, is $\pm 0.03 \text{ kW/m}^2$ during a test. Data logger resolution, item 3, for a ± 50 millivolt scale is 3.33 microvolts. Time dependent variations relate to thermocouple response and data logger clock precision. Thermocouple response is primarily related to temperature lag during a rising or falling temperature condition. This temperature lag, item 4, is estimated to be on the order of 0.25 s [7]. The data logger input sample rate, item 5, is 18.8 milliseconds per channel with a clock error of one minute per month [8].

Test repeatability was studied by conducting eight replicate tests on a typical fire fighter protective clothing garment assembly. The test specimen consisted of an 0.254 kg/m^2 (7.5 oz/yd) flame resistant fabric shell, a nonbreathable moisture barrier and a quilted thermal liner. These tests were carried out at a total heat flux level of 2.5 kW/m^2 . It is estimated from these tests that the overall temperature variation for the front surface thermocouple and the back surface thermocouple is about $\pm 5^\circ\text{C}$ ($\pm 9^\circ\text{F}$). See figures 14 and 15. Variations for the center thermocouple were within $\pm 8^\circ\text{C}$ ($\pm 14^\circ\text{F}$). See figure 16. This increased variation is attributed to each of the different thermocouples being located between assembly layers that possessed different degrees of garment loft or air space that existed between the garment layers.

In addition to the above experiments, the need for fast response was compared to thermocouple functional performance. Thermocouples made from a range of wire diameters, 0.127 mm (0.005 in) to 0.635mm (0.025 in), were studied. The smallest diameter thermocouple has the fastest response time, estimated to be 0.1 s [7], as compared to the other thermocouples. However, this very fine thermocouple wire was difficult to use. A significant factor contributing to selecting the 0.254 mm (0.010 in) diameter thermocouple wire for use with this test was that the smaller diameter thermocouple wire broke easily. Thermocouple beads on the 0.127 mm (0.005 in) wire would break and welds that joined the thermocouples to data lead wire were also easily broken. Mechanical failures from the smaller diameter wire had a negative impact on test operations. Mechanical performance also had a negative impact on the use of thermocouples made from wire sizes larger than 0.254 mm (0.010in). Thermocouples made from larger diameter wires were relatively stiff, and stiffness made it difficult to attach thermocouples to fabric without causing deformation of the fabric layer. Also, larger diameter thermocouple wires diminish precision by increasing measurement response times, and larger thermocouple bead sizes increase errors associated with thermal radiation heat loss.

A thermal radiation heat loss error study was conducted to further evaluate precision of thermocouple junctions made with 0.254 mm (0.010 in) wire. This study was conducted at a heat flux of 5 kW/m^2 and used three different type K thermocouple wires sizes and bead sizes. See the data plots for one of these tests in figure 17. These plots show temperature measurements on the specimen's front surface directed toward the radiant heat source. The thermocouple wire diameters used were 0.254 mm (0.010 in), 0.508 mm (0.020 in) and 0.635mm (0.025 in). A micrometer was used to measure the thermocouple beads formed by these different wire sizes. Each thermocouple bead was measured a minimum of five times. The average diameter for each thermocouple bead was calculated to be 0.635 mm (0.025 in), 0.889 mm (0.035 in), and 1.372 mm (0.054 in) respectively.

Results from these tests show that the 0.254 mm (0.010 in) thermocouple wire had the fastest response and produced the highest temperatures. This is attributed to its smaller mass and bead diameter. Using thermocouple temperature values from the steady state part of figure 14, a thermal radiation correction of +2.5°C (+4.5°F) was estimated for the 0.254mm (0.010 in) thermocouples. This radiation error represents a temperature correction of 2 percent.

5.0 TEST DESCRIPTIONS AND RESULTS

The protective clothing specimen assemblies as described in section 3.2.2 were exposed to three basic heat flux exposures: low, medium and high levels of heat flux. These basic exposures relate to fire fighting environments identified during the "Project Fires" study [9] and studies reported by NIST [3]. The low heat flux level exposure, 1 kW/m^2 , represents an environment where a fire fighter is functioning some distance away from a fire and only a small quantity of external heat energy is experienced. The medium level exposure, 2.5 kW/m^2 , relates to a fire fighter that is relatively close to a fire and is likely to be actively engaged in fire fighting. And, the high heat flux level, $>20 \text{ kW/m}^2$, represents a fire fighter that is caught in a room flashover. The term flashover as defined by ASTM [10] is: "The rapid transition to a state of total surface involvement in a fire of combustible materials within an enclosure." The discussion further defines flashover in the following way [10]: "Flashover occurs when the surface temperatures of an enclosure and its contents rise, producing combustible gases and vapors, and the enclosure heat flux becomes sufficient to heat these gases and vapors to their ignition temperatures. This commonly occurs when the upper layer temperature reaches 600°C or when the radiation heat flux at the floor reaches 20 kW/m^2 ."

Figure 11 shows thermocouple locations for data graphs in figures 18 through 22. Figure 12 shows thermocouple locations for data graphs in figures 23a, 23b, and 23c. All of these preliminary tests had three thermocouples attached to the specimen as described in section 3.3.2, except no mid-point thermocouple was used.

It is important to note that this report has been written to document apparatus and measurement methods that may be used for evaluating the thermal performance of fire fighters' protective clothing. No attempt has been made to predict exposure times related to the development of burn injuries. Predicting thermal conditions that can cause a burn injury is a complex issue, and it is being addressed in other NIST measurement and modeling studies. However, results produced by this test methodology do provide detailed comparative data on the thermal performance of fire fighters' protective clothing while exposed to various environmental conditions. These data are being used to assist in evaluating computer models that are under development for predicting the thermal performance of fire fighters' protective clothing. In addition, these data may also be used by computer based methods for predicting burn injury potential. Burn injury prediction methods may be found in ASTM standards C 1055 and C1057 [11][12]. Also see studies conducted by Alice Stoll, et al. [13][14], Moritz and Henriques [15], and F.S. Knox, et al. [16]. Stoll and Chianta [13] provide basic background information on human skin burn injuries. They state in their study that the severity of a skin burn injury depends upon the elevation of human tissue temperature to a level

higher than 44°C (111°F) and that severity of a burn injury is an inverse relationship of time to tissue temperature. They also state that the rate at which a burn injury proceeds increases logarithmically with a linear increase in skin temperature so that at a skin temperature of 50°C (122°F) damage proceeds at 100 times the rate ensuing at 45°C (113°F). Research by Stoll and Greene [14] shows that when human skin reaches a temperature of 55°C to 60°C (131°F to 140°F) a second degree burn will occur. This type of burn injury causes blisters and complete destruction of the epidermis. A second degree burn injury is considered to be serious [11].

It is important that the reader understand that temperatures presented in this report are not human tissue temperatures. The temperatures are from thermocouples attached fire fighters' protective clothing fabrics, and simple attempts to estimate the potential for burn injury from these data may be misleading.

5.1 1.0 kW/m² HEAT FLUX TESTS

The first test exposures using this test apparatus were carried out with a radiant heat flux level of 1 kW/m². This exposure represents an intense solar heat flux or a condition where a fire fighter has entered a building and is located down a corridor from a burning room. The burning room is emitting flames into the corridor and for a short distance along the corridor's ceiling. This scenario is discussed in reference [3]. Each of the tests were conducted for a period of at least 600 s. This allowed for the temperature measurements to exhibit a steady-state condition. Results from these tests demonstrated the utility of the test method; however, it was apparent that a higher radiant heat flux level was needed to make comparisons between wet and dry test specimens. An example of test data from a 1 kW/m² test is shown in figure 18. Figure 11 shows thermocouple locations for data plots on figure 18. Note that these data plots show that the thermocouple located on the back surface of the thermal barrier fabric behind the retroreflective trim has a lower temperature than the thermocouple located on the back surface of the thermal barrier fabric beside the trim.

5.2 2.5 kW/m² HEAT FLUX TESTS

The 2.5 kW/m² thermal radiation exposure was used to simulate a condition where the fire fighter mentioned in section 5.1 has moved down the corridor, closer to the burning room [3]. Figures 19, 20, and 21 show data plots generated from three 2.5 kW/m² tests. Figure 19 shows results from a dry protective clothing test assembly that consisted of an aramid shell fabric, a nonbreathable moisture barrier, and an aramid quilted batting thermal liner. These data show that a thermal radiation exposure of only 2.5 kW/m² can cause a significant increase in protective clothing temperature. Also, data generated from a series of dry protective clothing tests were used to evaluate a first generation computer based mathematical model for predicting the thermal performance of fire fighters' protective clothing. Information on this thermal performance computer model is contained in NISTIR 6299 [4].

In addition to the dry protective clothing assembly test described above, two tests were conducted with wet protective clothing assemblies. The first wet test used 38 ml of distilled water sprayed

across the back surface of the thermal liner, figure 20. This specimen was extremely wet, and moisture dripped from the specimen as it was attached to the test specimen trolley. As can be seen, the moisture on the thermal liner kept the garment temperature down until it evaporated. Upon drying, the thermocouple temperatures increased rapidly. On the second wet test shown in figure 21, only 25 ml of water was used to wet the specimen's thermal liner. In this test, no water dripped from the test specimen before or during the test. Note that the reduced amount of water resulted in a reduced time period before the temperature rapidly increased. This shows that moisture content is an important part of the ensemble's ability to protect from burns. This is uncontrolled. In situations where the thermal liner dries out, rapid and possibly unexpected increases in temperature can occur resulting in burns.

5.3 RADIANT HEAT FLUX TESTS WITH FLAMES

The radiant heat flux tests with the addition of flames were selected to represent a fire fighting scenario where a fire fighter is exposed to a thermal radiation environment and is suddenly struck by a flame. The first tests using radiant heat energy and flame contact were conducted with a radiant heat flux of 1.0 kW/m^2 . An example of these tests is shown in figure 22. The protective clothing specimen assembly used in this test consisted of a trim material with a reflective surface made of glass micro-beads, aramid shell fabric layer, nonbreathable moisture barrier, and a quilted aramid batting thermal liner. Thermocouple locations for this test are shown in figure 11. Thermocouple (1) is the front surface measurement location, thermocouple (2) is located on the back surface behind the trim, and thermocouple (3) is located on the back surface in the open field beside the trim. The flame height was adjusted to cover the entire height of the test specimen, and the burner was applied to the specimen at 360 seconds into the test. The radiant flux plus the flame created a total heat flux of approximately 30 kW/m^2 to 40 kW/m^2 . The flame was left in contact with the test specimen for 60 seconds. The gas pilot flame was then removed and extinguished. The glass micro-bead trim material showed no flaming combustion after the pilot flame was removed. In addition, tests of a trim made with a reflective surface of prisms formed in a flexible polymer material also self-extinguished after the pilot flame was removed.

A similar flame exposure test was conducted using an initial heat flux of 2.5 kW/m^2 , shown in figures 23a, 23b, and 23c. This test was carried out using a protective clothing specimen assembly consisting of a glass micro-bead trim material, an aramid shell fabric layer, breathable moisture barrier, and a quilted aramid batting thermal liner. Thermocouple locations for these figures are shown in figure 12. Figure 23a represents data from the top pair of thermocouples shown on the thermal liner's back surface. Figure 23b represents the center set of thermocouples, and figure 23c presents results from the bottom set of thermocouples on the thermal liner's back side. In this test, the 2.5 kW/m^2 radiant flux exposure was maintained for a period of about 160 seconds before a flame was applied to the test specimen. The initial exposure was designed to simulate a fire fighter entering a building just prior to flashover. At the 160 second point, the test specimen was quickly moved forward on its trolley to a point pre-calibrated to give an exposure of 20 kW/m^2 , and the flame was placed into contact with the test specimen. The combination of thermal radiation from the radiant panel and flame contact produced a mean total heat flux of about 50 kW/m^2 with a heat

flux range of 40 to 60 kW/m². The fluctuation in heat energy is attributed to exposure flame variability. This high heat energy exposure simulates conditions when a fire fighter is caught in a flashover environment. The three thermocouple plots shown in figures 23a, 23b, and 23c again demonstrate the thermal performance of the protective clothing assembly. The difference between the front surface thermocouple temperature and the back surface thermocouple temperatures provide information on the garment's thermal insulating characteristics. Note that the rate of temperature rise for thermocouple (3) changes rapidly at about 130 seconds. The time lag between rapid temperature rise for the front surface thermocouple and rapid temperature rise of the back surface thermocouple (3) beside the trim was approximately 15 seconds. Rapid temperature rise for the thermocouple located behind the trim (2) didn't occur until about 20 seconds after the front surface thermocouple began its rapid change in temperature. The thermocouple behind the trim (2) indicates that the trim provided additional thermal protection. Another interesting observation on this data plot is that the temperature on the back side of the protective clothing peaks and begins to drop while the flame is still being applied to the test specimen. This may indicate that a portion of the temperature rise measured on the specimen's back side resulted from test specimen combustion. Cooling of the back surface thermocouples, while the flame is still being applied, may indicate that combustion of the protective clothing specimen materials has ended and that the charred material is providing insulation. This phenomenon is not apparent with data shown in figure 22 for the lower heat flux exposure.

5.4 OPEN AND CLOSED BACK SPECIMEN TESTS

After completing the tests discussed above, an additional series of tests was conducted to further develop the test apparatus and method. These tests were primarily conducted to compare results from open back and closed back specimen holders. The two specimen holder configurations are shown in figure 8. As seen in figure 8, the closed back test specimen assembly used a 6.4 mm (0.25 in) thick aluminum plate spacer between the specimen's back surface fabric and the closure. This spacer was included to provide a constant space that would simulate, to some degree, garment ease. It is estimated that garment space or ease in protective clothing will vary from direct contact to approximately 13 mm (0.5 in). In addition to the change already discussed, five thermocouples were attached to the test specimens to better resolve test performance. Four of the thermocouples were attached as discussed in section 3.2.1. One additional thermocouple was sewed to the back of the shell fabric along the centerline directly behind the trim. A sketch showing the location of all thermocouples used in this test series is shown in figure 13.

This series of tests was conducted with a heat flux of 2.5 kW/m². These tests were carried out to investigate the thermal effects of open backed specimen assemblies as compared to closed back specimen test assemblies. Tests were run with dry and wet protective clothing specimens. The tests employed two protective clothing assemblies that represent fire fighter protective garments currently being used by the fire service. These protective clothing assemblies used different retroreflective trim products manufactured by two different manufacturers, and the trim was professionally sewed to a single type of woven flame resistant protective clothing shell fabric. The test specimens used two different moisture barrier systems that are commercially produced. These moisture barriers

represented both permeable/breathable and impermeable/non-breathable systems. The thermal liner used in all of the test specimen assemblies consisted of a flame resistant non-woven batting sewn, using a quilt pattern, to a flame resistant woven liner fabric. Figures 24 through 31 present data plots from these tests. Of these data plots, figures 24 through 27 show test results from protective clothing specimens tested dry. Figures 28 through 31 show test results from protective clothing specimens tested wet. In these tests, 10 g of distilled water was sprayed across the back side of the shell fabric, and 10 g of water was sprayed onto the woven fabric side of the thermal liner. This amount of water represents a moisture coverage of 155 g/m^2 (4.6 oz/yd^2) on the shell fabric and also on the thermal liner. As a comparison, Malley [17] reported on a study that measured sweating rates of fire fighters while they were wearing their protective clothing ensemble and exercising. This study indicated that a fire fighter's maximum sweating rate may be slightly greater than 2.3 l/hr , which is approximately equivalent to 2300 g/hr (81 oz/hr). This sweating rate, if evenly distributed over the area of a nominal medium sized thermal liner of a fire fighter's protective garment constructed from 3.34 m^2 (4 yd^2) of fabric, would create a moisture coverage of 155 g/m^2 (4.6 oz/yd^2) in about 13.5 minutes.

Results from these tests show that temperatures throughout the specimen are generally higher with the closed back test specimen assemblies. These higher temperatures were expected since the closed back tests reduced heat loss from the specimen. Test results from the dry specimens show only moderate increases in temperatures throughout the garment specimen assembly. When the specimens were tested wet, there was a significant difference in temperatures between the open back and closed back tests. The noteworthy lower temperatures in the wet open back protective clothing systems are attributed to the free evaporation of moisture from the specimen assemblies. Additionally, there are some significant differences recognized when comparing the permeable and impermeable moisture barrier protective clothing systems. These differences are easily seen when comparing temperatures for thermocouple (3), (4), and (5) in figures 28 through 31. All of these thermocouples are located on the thermal liner. Thermocouple (3) is located on the inside surface of the thermal liner that faces the moisture barrier and directly behind the impermeable trim on the shell fabric. Thermocouple (4) is located on the thermal liner's back side that would be closest to the fire fighter's skin or work uniform, and it is located directly behind the impermeable trim. Thermocouple (5) is located on the thermal liner's back side as with thermocouple (4), except that it is located in the open field beyond the impermeable trim's edge. When comparing data plots for thermocouples (3),(4), and (5) in figures 28 through 31, it is apparent that some different heat transfer process is taking place. In figure 31 with the permeable moisture barrier, thermocouples (3) and (4) rise rapidly to a relatively high temperature as compared to that seen with the impermeable specimen shown in figure 29. In addition thermocouple (5), figure 31, located in the garment specimen's open field increases at a slow rate. The rate of temperature increase for thermocouple (5) in figure 31 exhibits a slow rate of change similar to the increase seen with thermocouples (3), (4), and (5) in figure 29 where an impermeable moisture barrier is used. This observation suggests that hot water vapors produced between the shell's impermeable trim and permeable moisture barrier expanded through the moisture barrier causing the temperature to rapidly increase on the woven fabric side of the thermal liner.

6.0 SUMMARY

This test apparatus will allow the thermal performance of fire fighters' protective clothing to be measured over a wide range of thermal exposures. This range may vary from the heat flux of a hot summer day to a post-flashover fire environment. The utility of this test apparatus is demonstrated by the detailed data that it produces. The data presents a clear graphical picture of how different protective clothing components perform under different thermal environment conditions. This type of measurement capability is currently not offered by any other thermal test methods for protective clothing. This test apparatus allows for measuring the performance of fire fighters' protective clothing at thermal environments far below those measured with the TPP test [1]. Reports from the fire service have indicated that many serious burn injuries are occurring in conditions much less severe than those specified by the TPP test. The TPP test method is limited by exposure time through the physical limits of its copper disk calorimeter and the short duration burn injury scale used for specifying the times for pain and burn injury [1]. The test apparatus and the procedures discussed in this report allow for protective clothing thermal performance to be measured over time periods that are significantly longer than those currently available with other test methods referenced by NFPA 1971. In addition, the thermal environment may be accurately varied during the test for evaluating the thermal performance of a protective clothing systems during dynamically varying fire fighting exposures. This is not possible with any of the currently available thermal performance test methods. This test apparatus may be used to measure the thermal performance of protective clothing systems in either a dry or wet state. Finally, test results are being used to evaluate the ability of computer models to predict the thermal performance of fire fighters' protective clothing [4].

7.0 FUTURE RESEARCH

The research addressed in this report provides new tools for measuring the thermal performance of fire fighters' protective clothing. They may be used to further develop an understanding of heat transfer through protective clothing and to better understand how moisture functions in thermal protective clothing. This apparatus, in its current design, will not provide appropriate measurements of protective clothing while being compressed. Addition work is needed to develop appropriate apparatus for measuring the thermal performance of protective clothing while being compressed. A need exists for measuring the compressed thermal performance of protective clothing when exposed to the following conditions: 1) while exposed to thermal radiation, 2) while compressed against a hot dry surface, and 3) while exposed to hot liquid covered surfaces. Each of these apparatus should be able to measure the thermal performance of protective clothing when it is wet or dry.

8.0 ACKNOWLEDGMENTS

The United States Fire Administration (USFA) partnered with NIST and co-sponsored this study. Appreciation is extended to Mr. Robert T. McCarthy, Chief, Fire Technical Programs Branch, USFA for his support, ideas and comments related to this project. Division Chief, Kirk Owen of the Plano, Texas Fire Department and Chairman of the NFPA Committee on the Protective Ensemble for Structural Fire Fighting was instrumental in encouraging this study. Fire Fighter Barry Borkowski, St. Andrews Fire Department, Manitoba, Canada is recognized for bringing questions concerning the performance of fire fighter's protective clothing to the NFPA committee. These critical questions had a significant impact on the direction of this research. Assistant Chief Charles Davis, Lexington, Kentucky Fire Department is recognized for the many discussions related to fire fighting environments and the performance of fire fighters' protective clothing. Mr. Don Aldridge, Vice President of Lion Apparel, Inc. and Ms. Patricia Freeman, Technical Service Manager, Globe Firefighters Suits, supplied test specimens used in the development of this study. Mr. Michael Stanhope, Ms. Denise Statham and Ms. Susan Tribble, Southern Mills, Inc. provided counsel on the properties of protective clothing fabrics and also provided test specimen materials. Appreciation is extended to Mr. Robert Vettori, of NIST, for preparing the data plots for this report.

9.0 REFERENCES

- [1] NFPA 1971, Standard on Protective Ensemble for Structural Fire Fighting, 1997 Edition, National Fire Protection Association, Quincy, MA.
- [2] Krasney, John F.; Rockett, John A.; Huang, Dingyi, Protecting Fire Fighters Exposed in Room Fires: Comparison of Results of Bench Scale Test For Thermal Protection and Conditions During Room Flashover, Fire Technology, National Fire Protection Association, Quincy, MA, February 1988.
- [3] Lawson, J. Randall, Fire Fighter's Protective Clothing and Thermal Environments of Structural Fire Fighting, NISTIR 5804, National Institute of Standards and Technology, Gaithersburg, MD, 1996.
- [4] Mell, William E. and Lawson, J. Randall, A Heat Transfer Model for Fire Fighter's Protective Clothing, NISTIR 6299, National Institute of Standards and Technology, Gaithersburg, MD, 1999.
- [5] American Society for Testing and Materials, E162 Standard Test Method for Surface Flammability of Materials Using a Radiant Heat Energy Source, Annual Book of ASTM Standards, Vol. 04.07, West Conshohocken, PA, 1997.
- [6] American Society for Testing and Materials, E1321 Standard Test Method for Determining Material Ignition and Flame Spread Properties, Annual Book of ASTM Standards, Vol. 04.07, West Conshohocken, PA, 1997.
- [7] Omega Engineering, Inc., The Temperature Handbook, Volume 29, Stamford, CT, 1995.
- [8] Campbell Scientific, Inc., 21X Datalogger Operator's Manual, Logan, UT, 1989.
- [9] Abeles, Fred J. and Himel, Victor, "Project Fires, Volume 2: Protective Ensemble Performance Standards, Phase 1B, Final Report," NASA - George C. Marshall Space Flight Center, Alabama, May 1980.
- [10] American Society for Testing and Materials, E176 Standard Terminology of Fire Standards, Annual Book of ASTM Standards, Vol. 04.07, West Conshohocken, PA, 1997
- [11] American Society for Testing and Materials, C1057 Standard Practice for Determination of Skin Contact Temperature from Heated Surfaces Using A Mathematical Model and Thermestesiotometer, Annual Book of ASTM Standards, Vol. 04.06, West Conshohocken, PA, 1997.

- [12] American Society for Testing and Materials, C1055 Standard Guide for Heated System Surface Conditions That Produce Contact Burn Injuries, Annual Book of ASTM Standards, Vol. 04.06, West Conshohocken, PA, 1997.
- [13] Stoll, Alice M. and Chianta, Maria A., Method and Rating System for Evaluation of Thermal Protection, Aerospace Medicine, Vol. 40 (11), pp. 1232-1237, November 1969.
- [14] Stoll, Alice M. and Greene, Leon C., Relationship between pain and tissue damage due to thermal radiation, Journal of Applied Physiology, Vol. 14, pp. 373-382, May 1959.
- [15] Moritz, A.R., and Henriques, Jr., F.C., "Studies of Thermal Injury II. The Relative Importance of Time and Surface Temperature in the Causation of Cutaneous Burns," America Journal of Pathology, Vol. 23, No. 5, 1947.
- [16] Knox, F.S. III; Bonetti, Dena; and Perry, Chris, "User's Manual for BRNSIM/BURNSIM: A Burn Hazard Assessment Model," USAARL Report No. 93-13, Air Force Systems Command Wright-Patterson Air Force Base, Ohio, United States Army Aeromedical Research Laboratory, Fort Rucker, Alabama, February 1993.
- [17] Malley, Kevin Lt., "The Influence of Protective Clothing on Firefighter - Health & Work Performance," Health and Safety Newsletter, Fire Department New York (FDNY), December 1996.



Figure 1 Photograph of test apparatus.

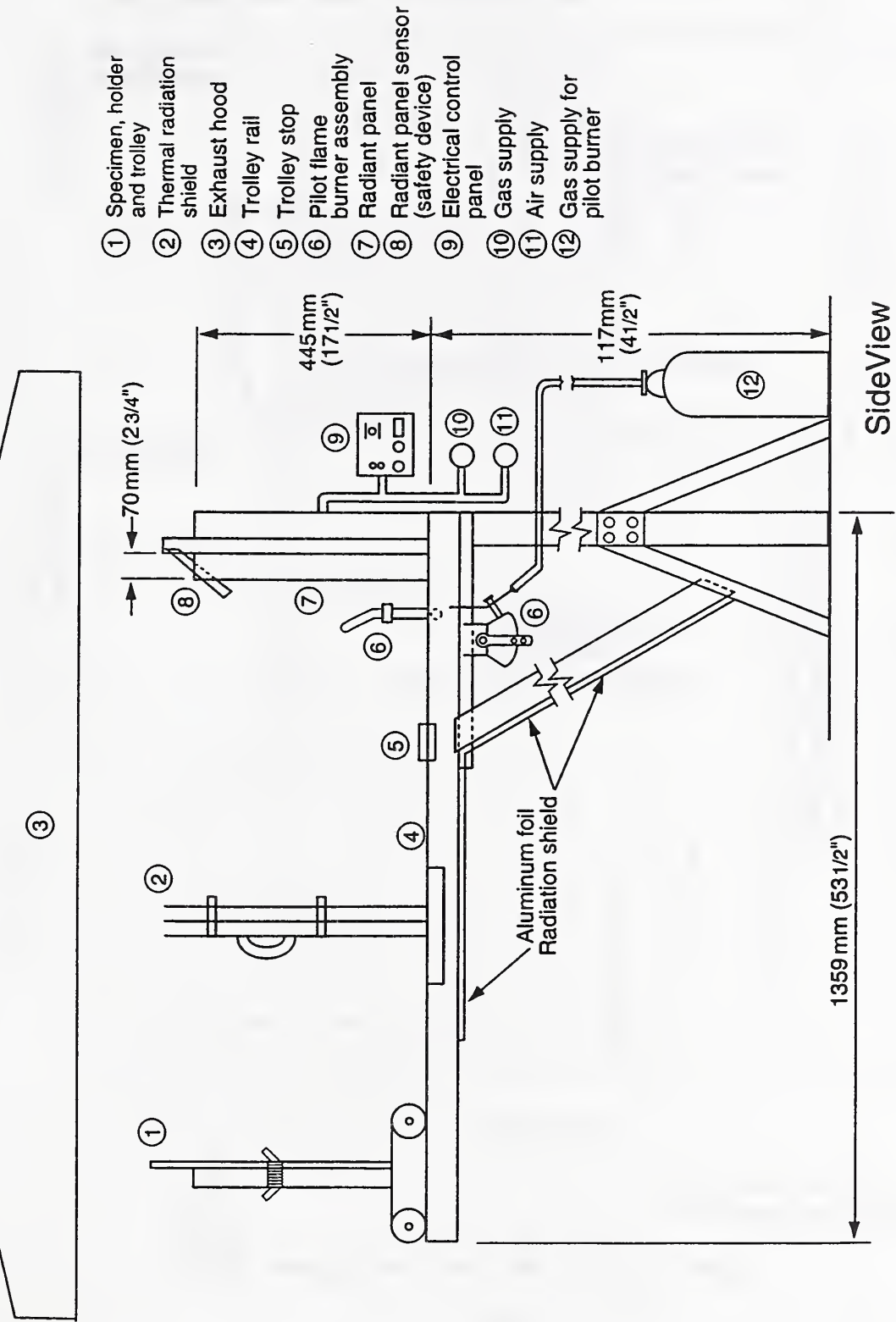
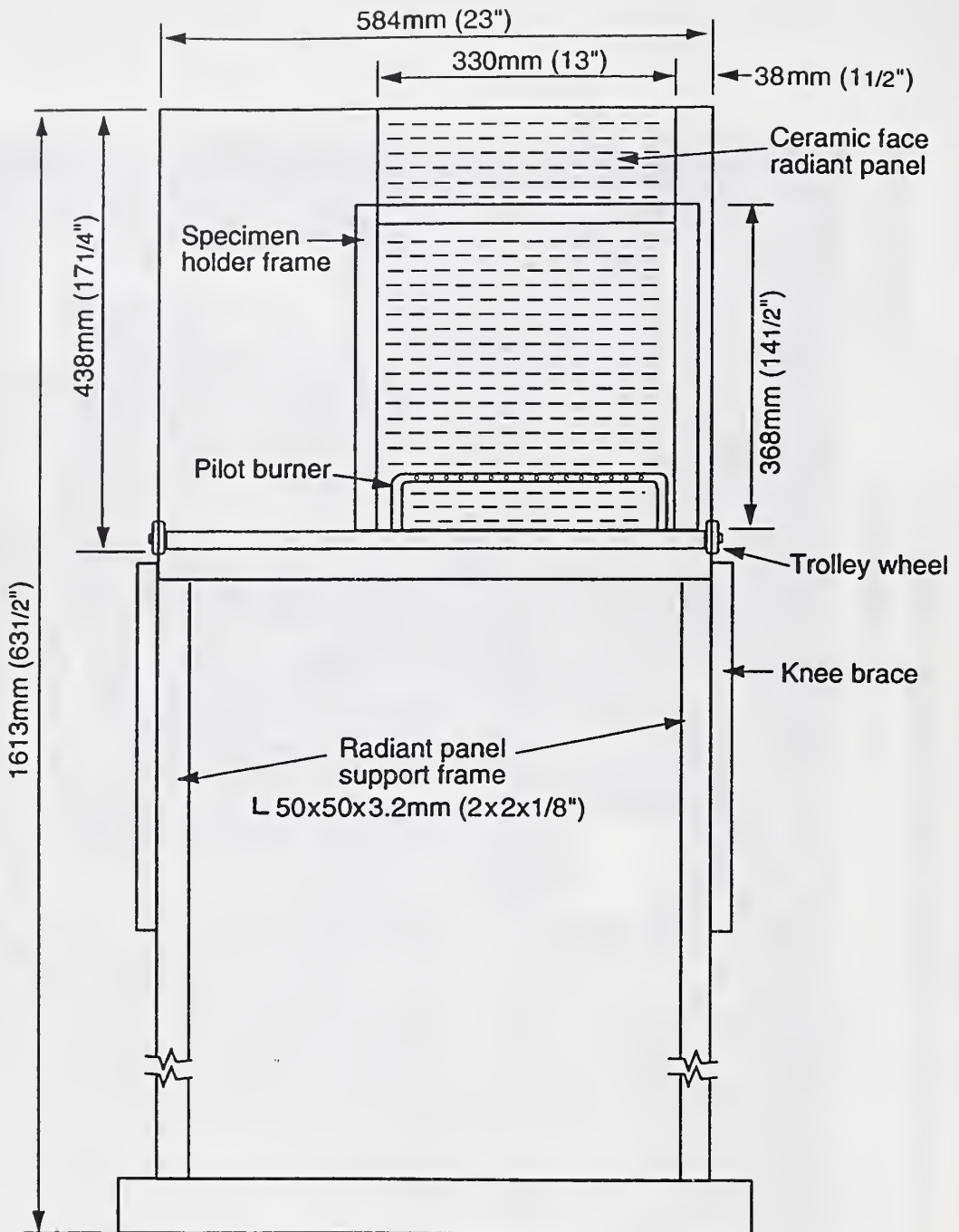


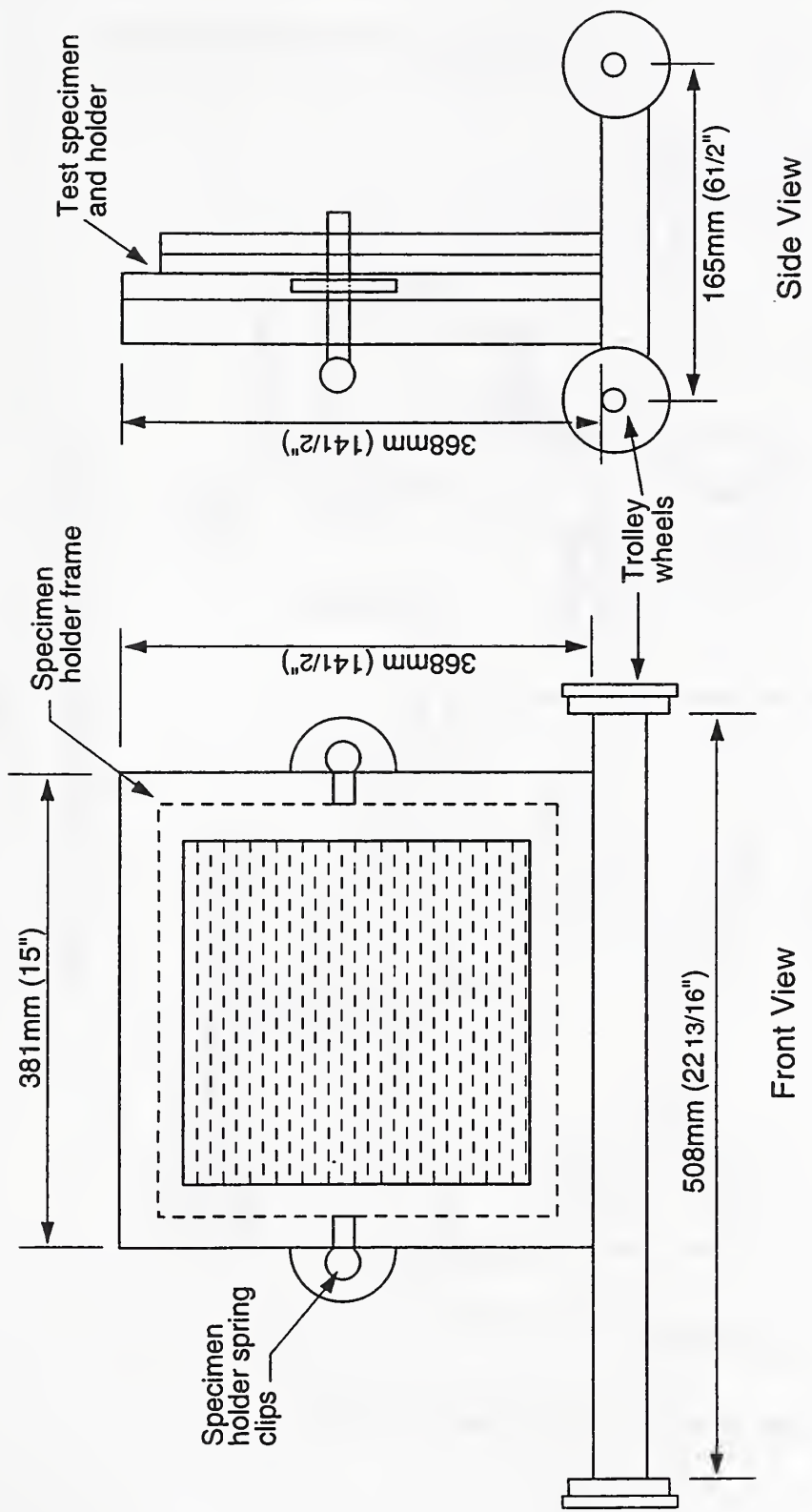
Figure 2 Sketch, side view of test apparatus.



Front View

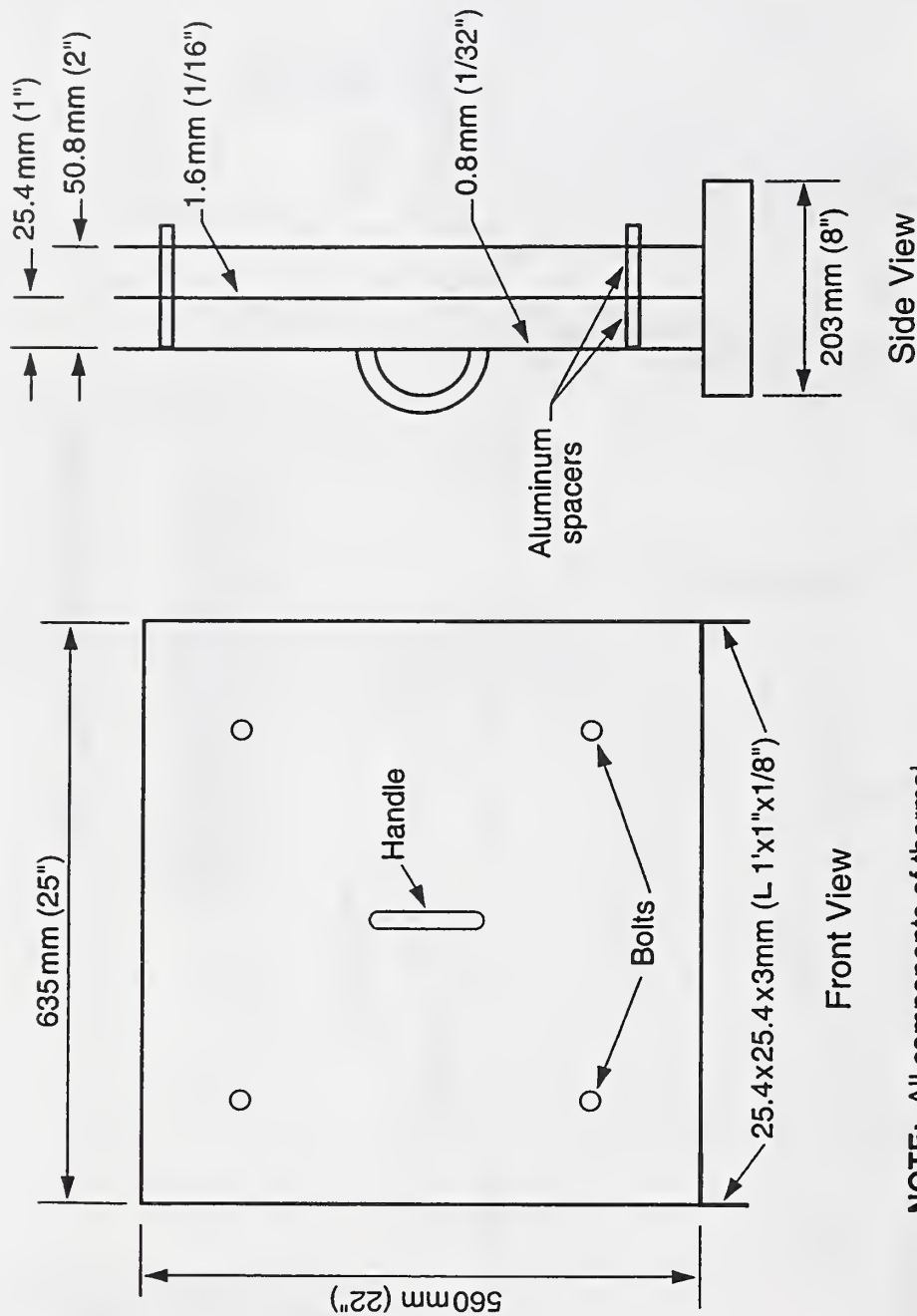
NOTE: Exhaust hood located
above test apparatus

Figure 3 Sketch, front view of test apparatus.



NOTE: All components except trolley wheels are made of steel, wheels are aluminum.

Figure 4 Sketch of trolley assembly



NOTE: All components of thermal radiation shield except the handle is made of aluminum.

Figure 5 Sketch of thermal radiation shield.

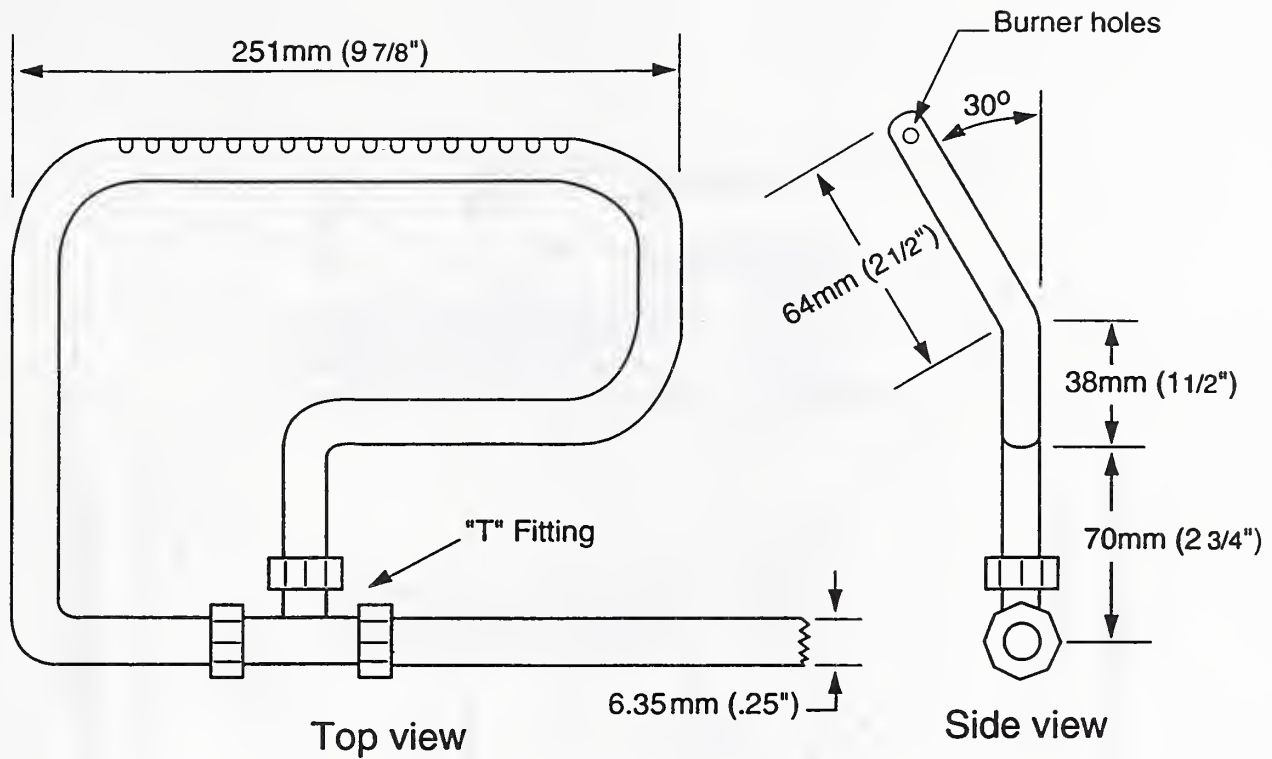


Figure 6 Sketch of pilot burner assembly.

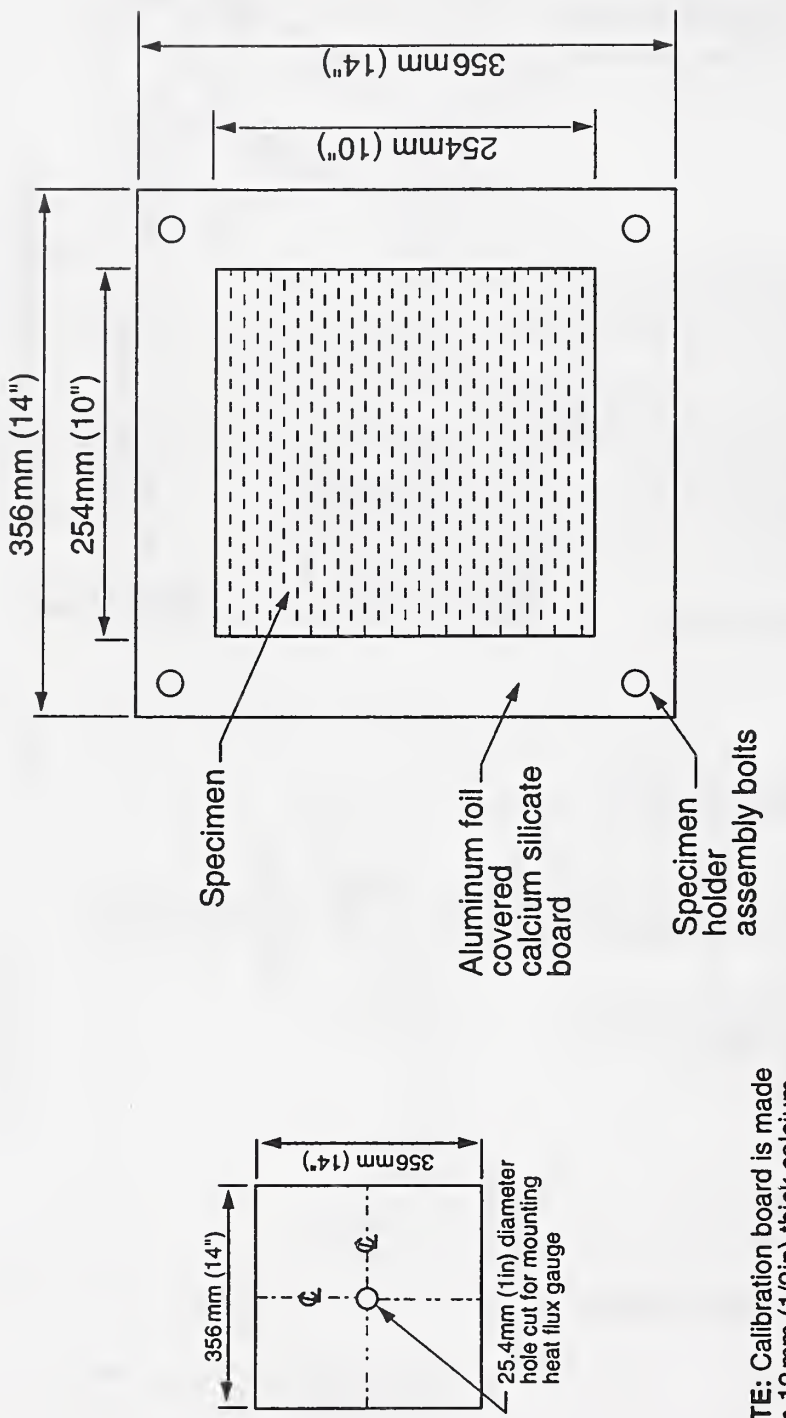
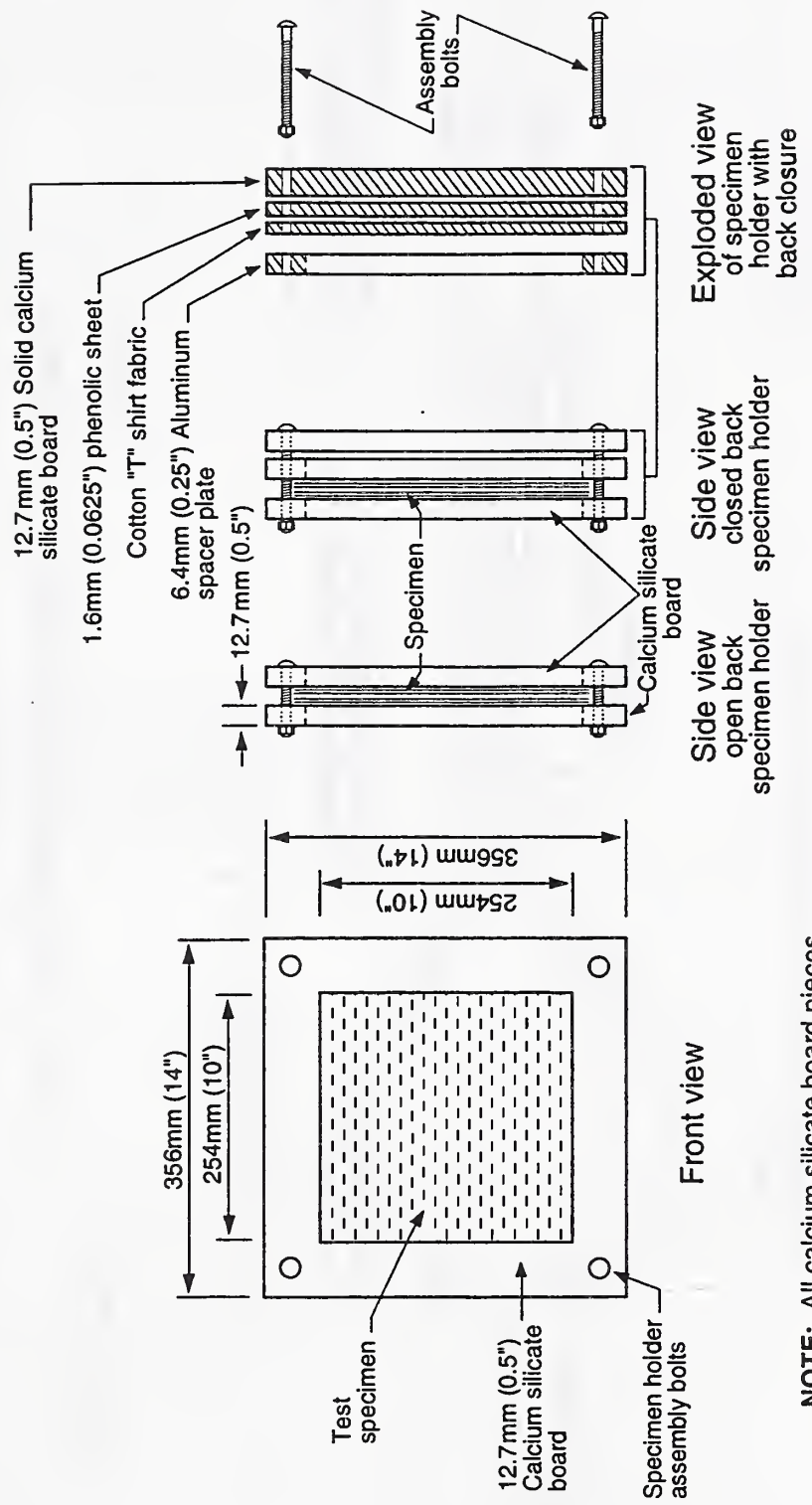


Figure 7 Sketch of calibration board and specimen holder.



NOTE: All calcium silicate board pieces except the back closure are covered with 0.05mm (0.002 in) thick aluminum foil. The back closure consisting of the phenolic sheet and calcium silicate board are covered with cotton "T" shirt fabric that is held in place on the closure's back surface with duct tape.

Figure 8 Sketch of open back and closed back specimen holders.

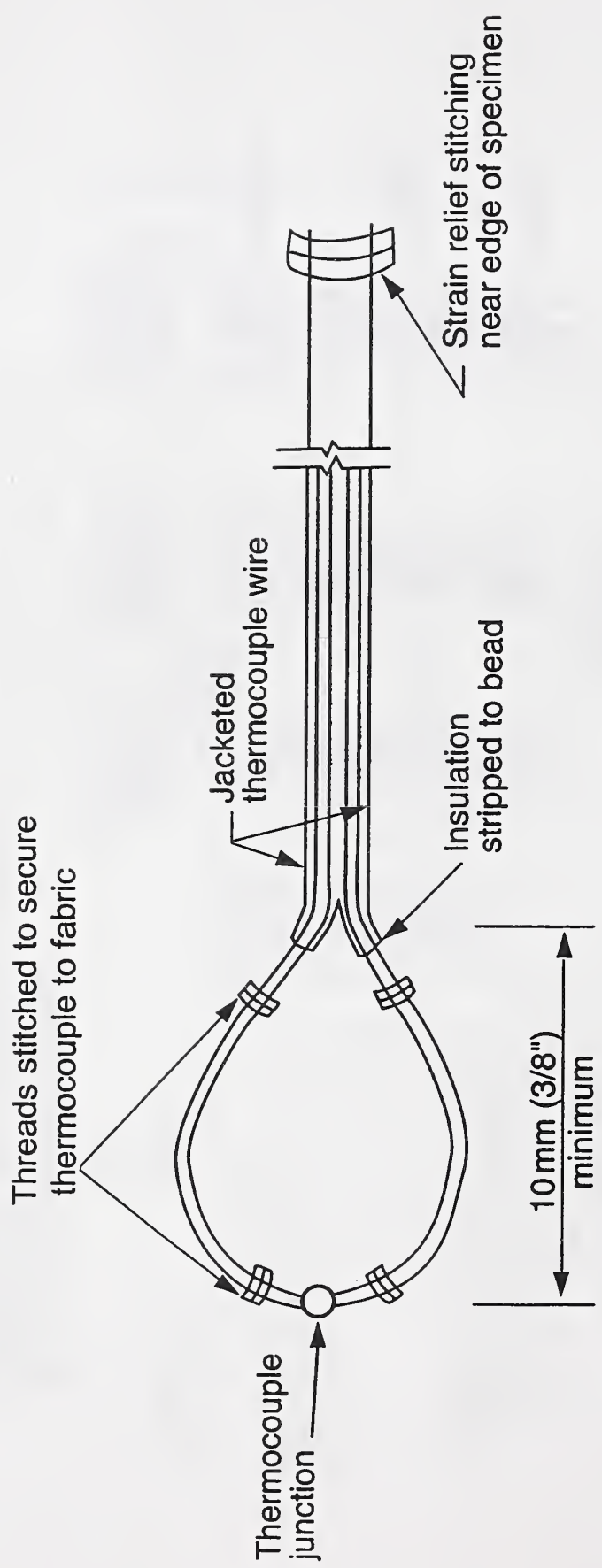


Figure 9 Sketch showing stitching for thermocouple attachment.

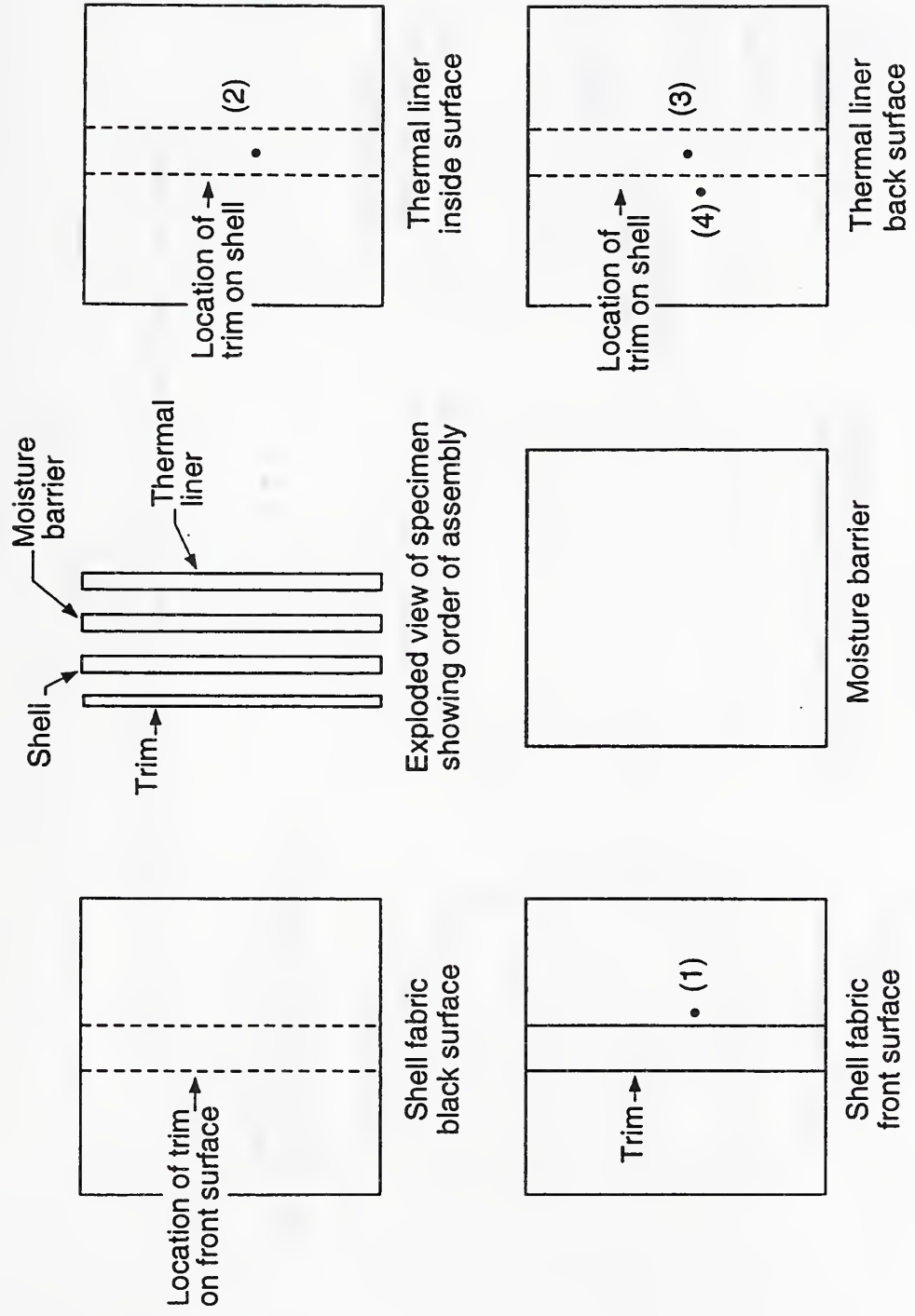
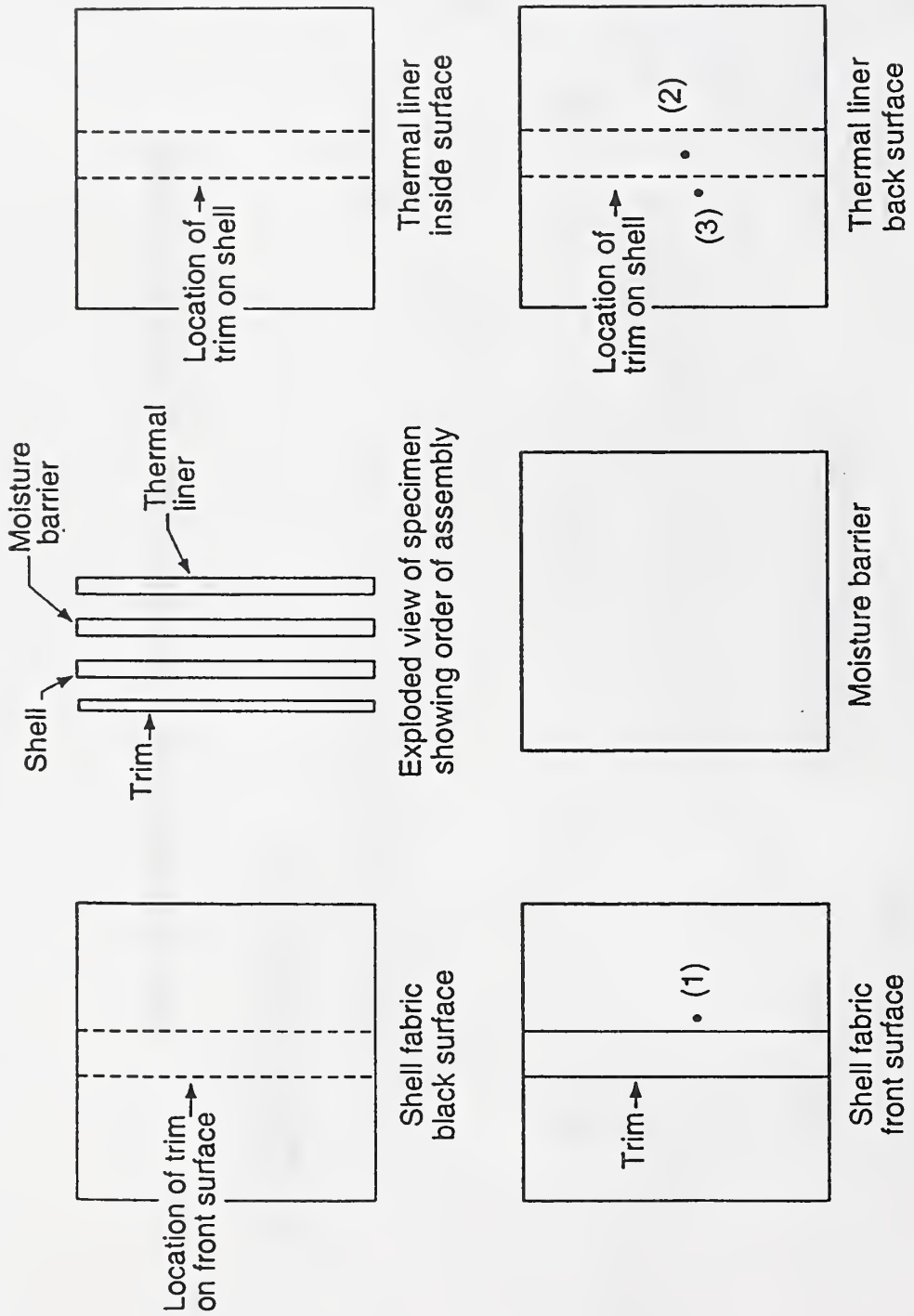


Figure 10 Recommended thermocouple locations used for standard testing.

- (#) Thermocouple location and identification number



- (#) Thermocouple location and identification number

Figure 11 Thermocouple locations used for data shown in figures 18 through 22.

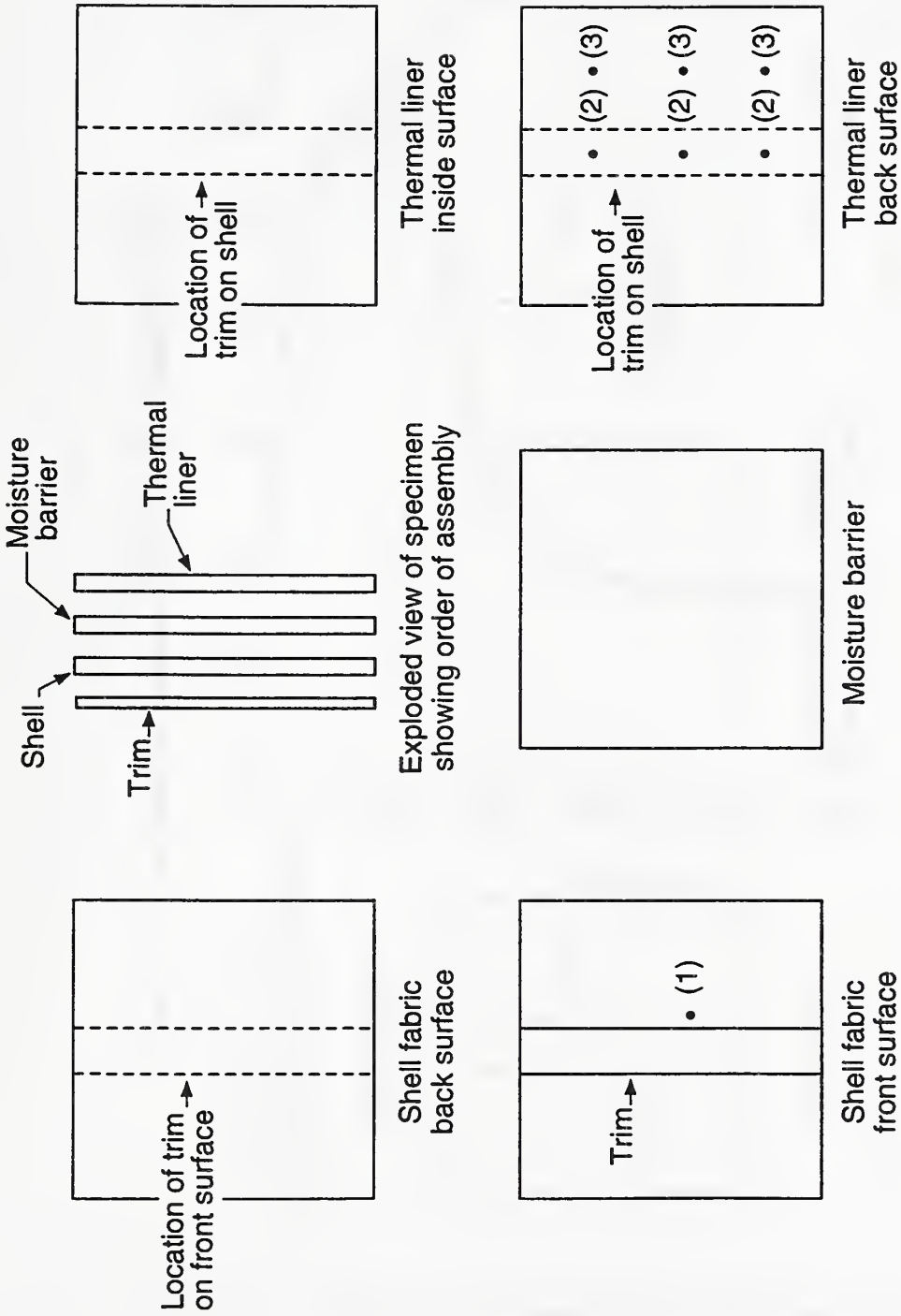


Figure 12 Additional thermocouple locations used for flaming exposures in figures 23a, 23b, and 23c.

- (#) Thermocouple location and identification number

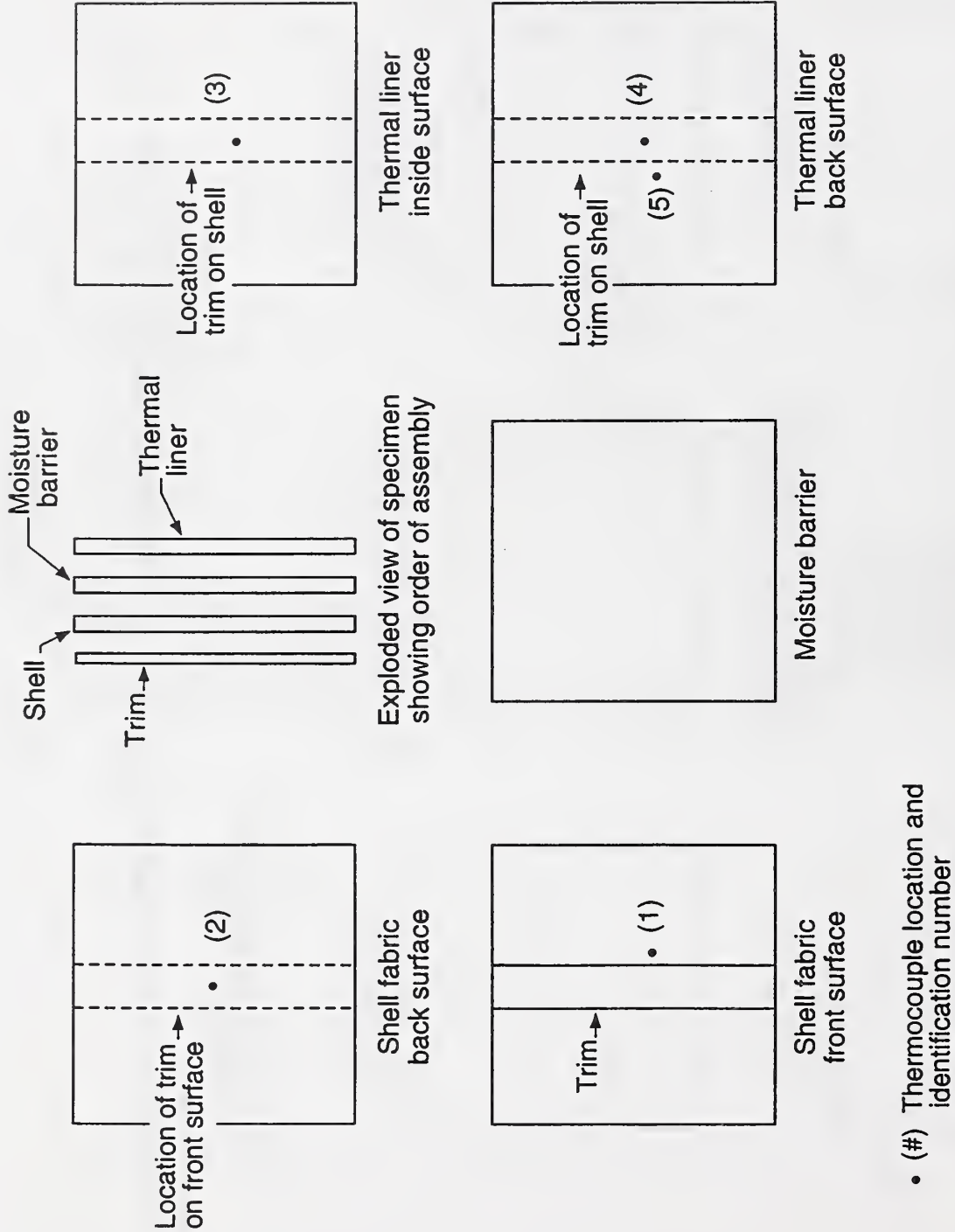


Figure 13 Thermocouple locations used with open and closed back tests.

- (#) Thermocouple location and identification number

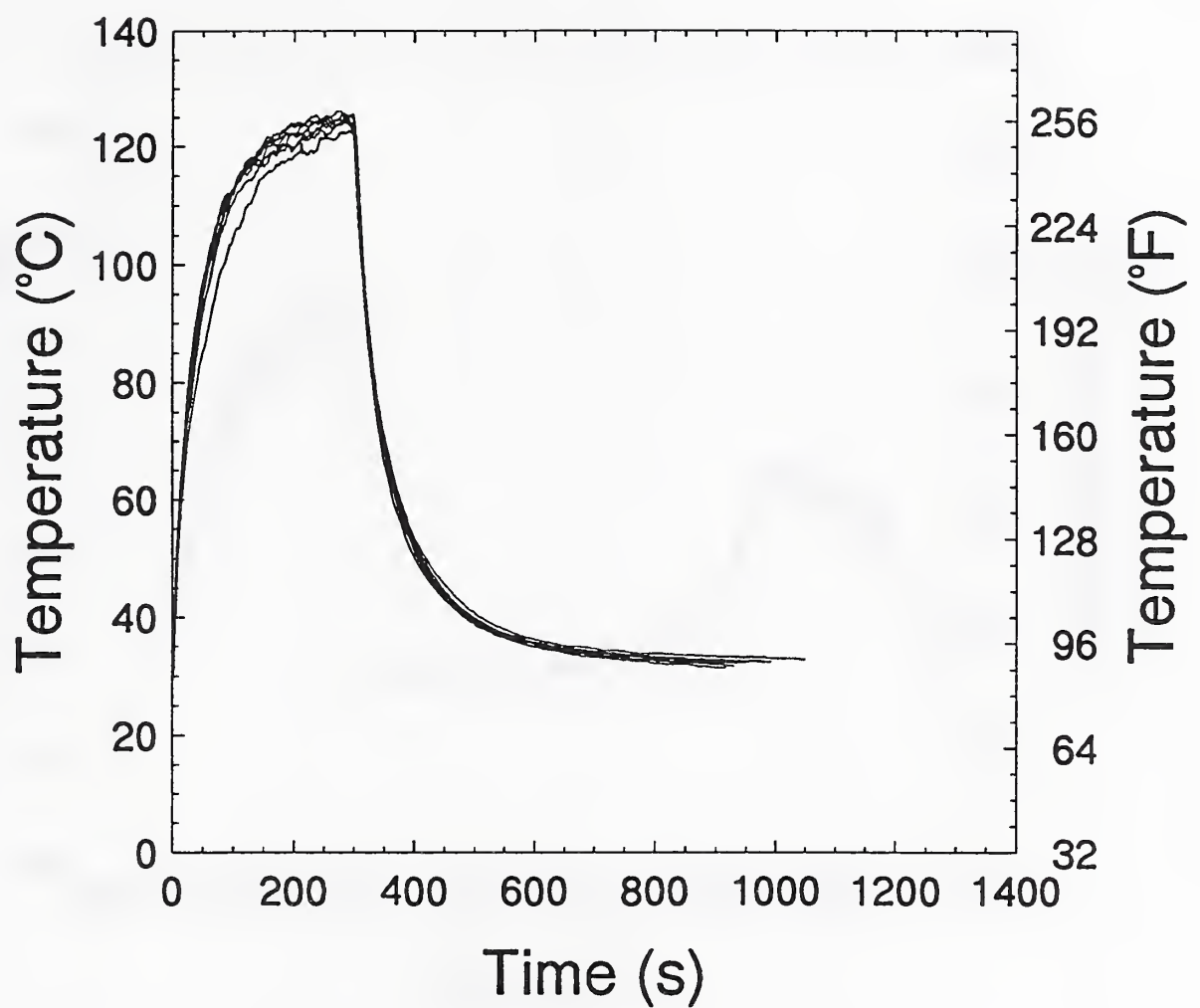


Figure 14 Variation of front surface thermocouple measurements for eight tests.

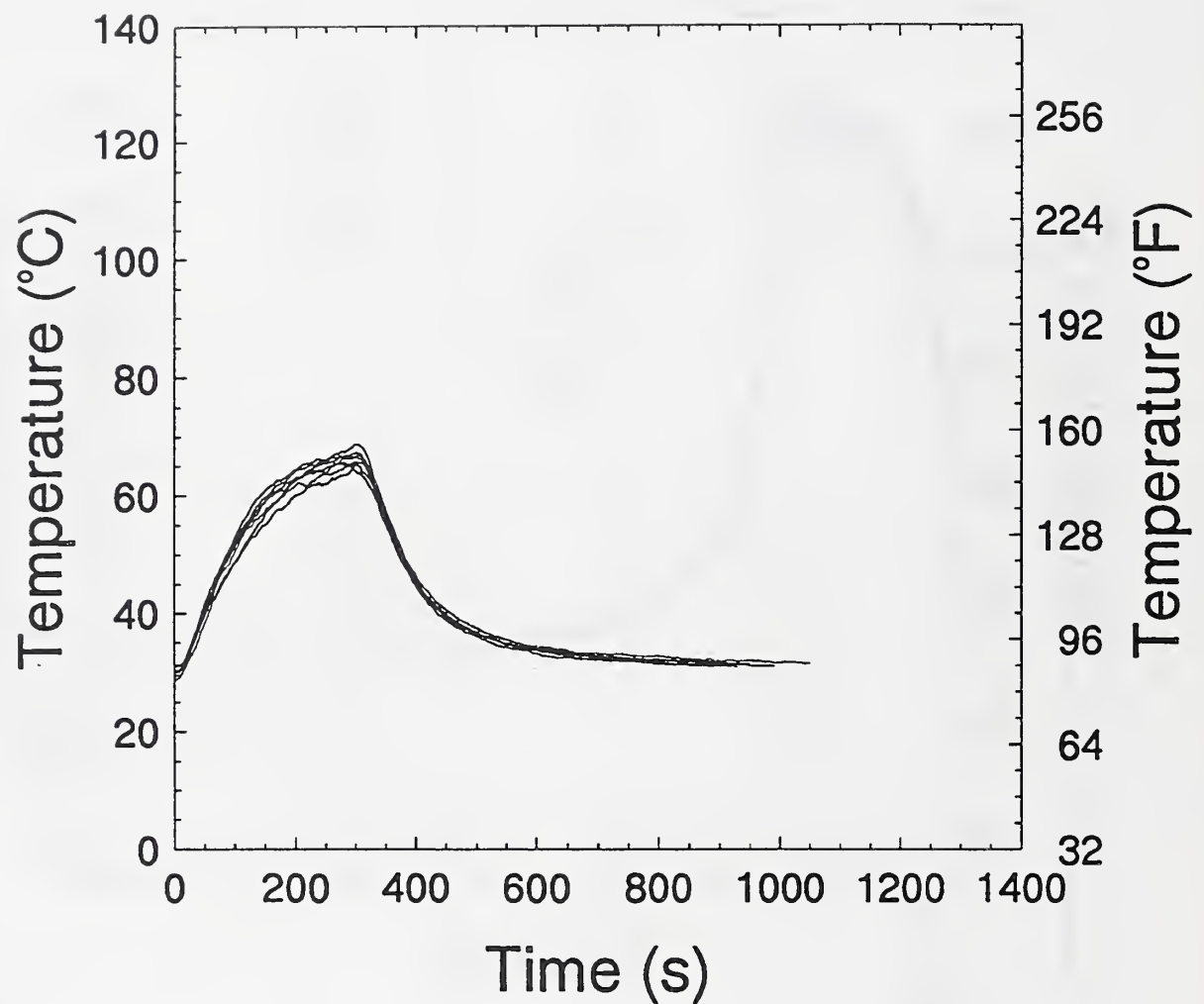


Figure 15 Variation of back surface thermocouple measurements for eight tests.

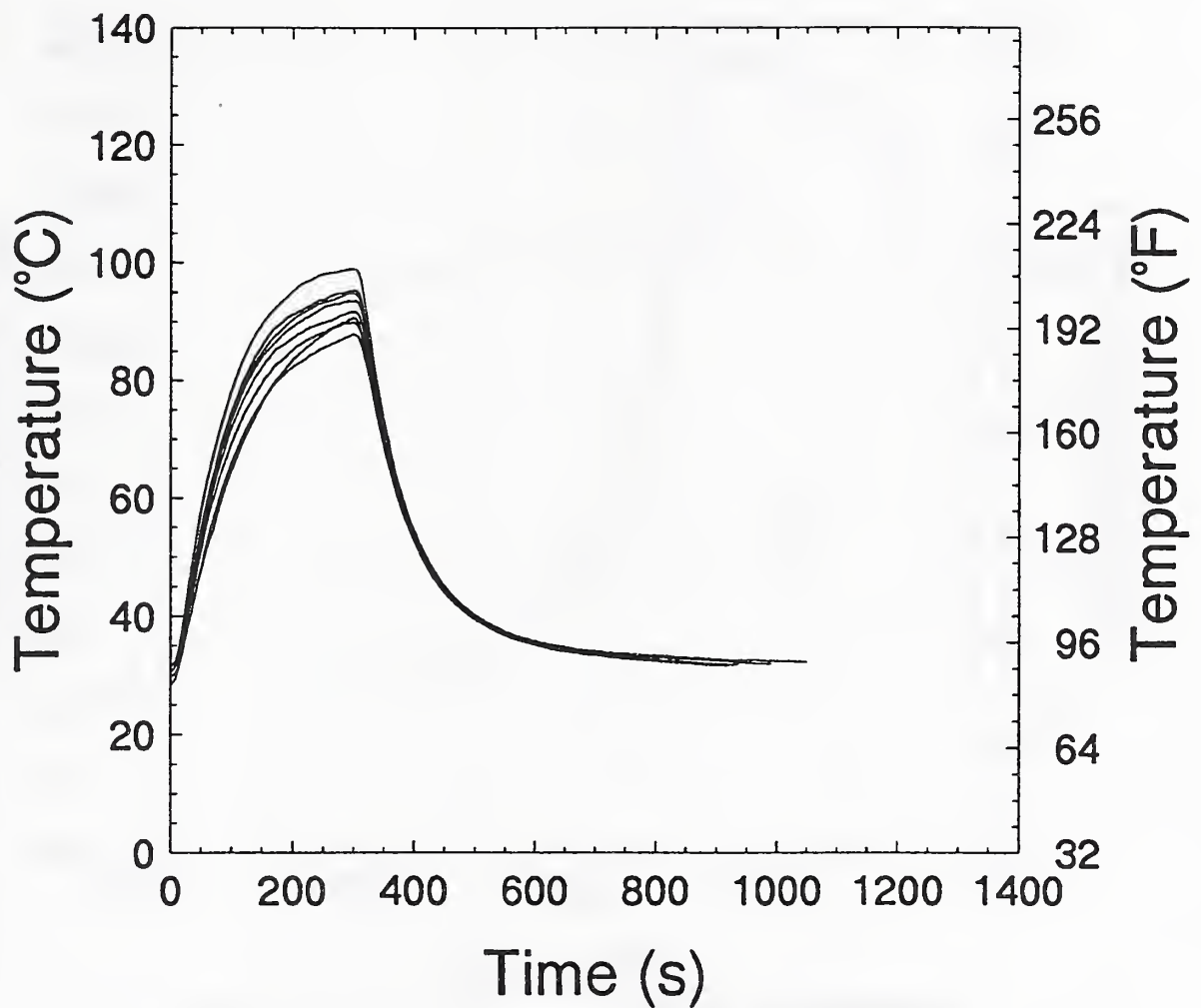


Figure 16 Variation of mid-point thermocouple measurements for eight tests.

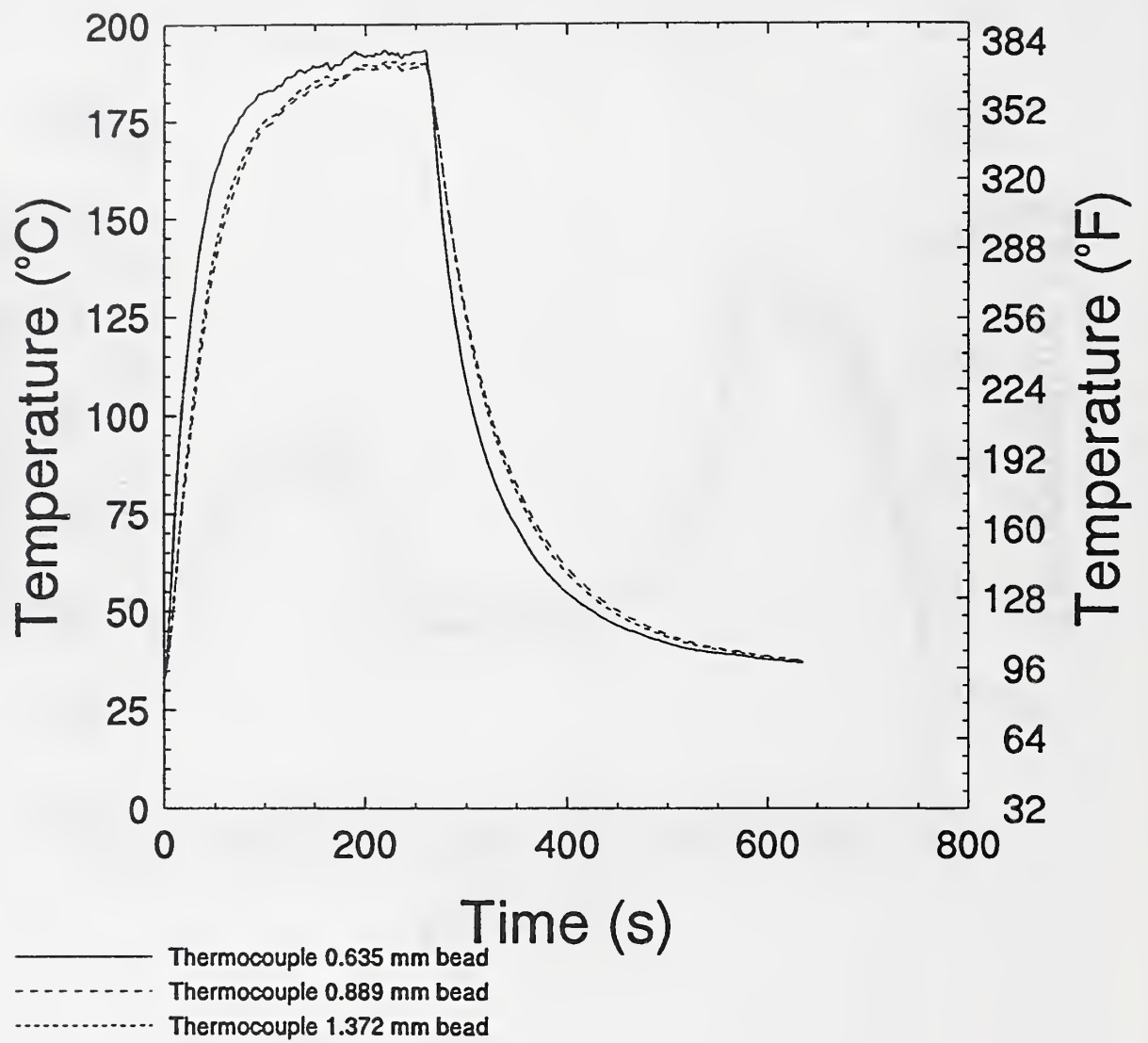


Figure 17 Data plots for thermocouple radiant heat flux error test.

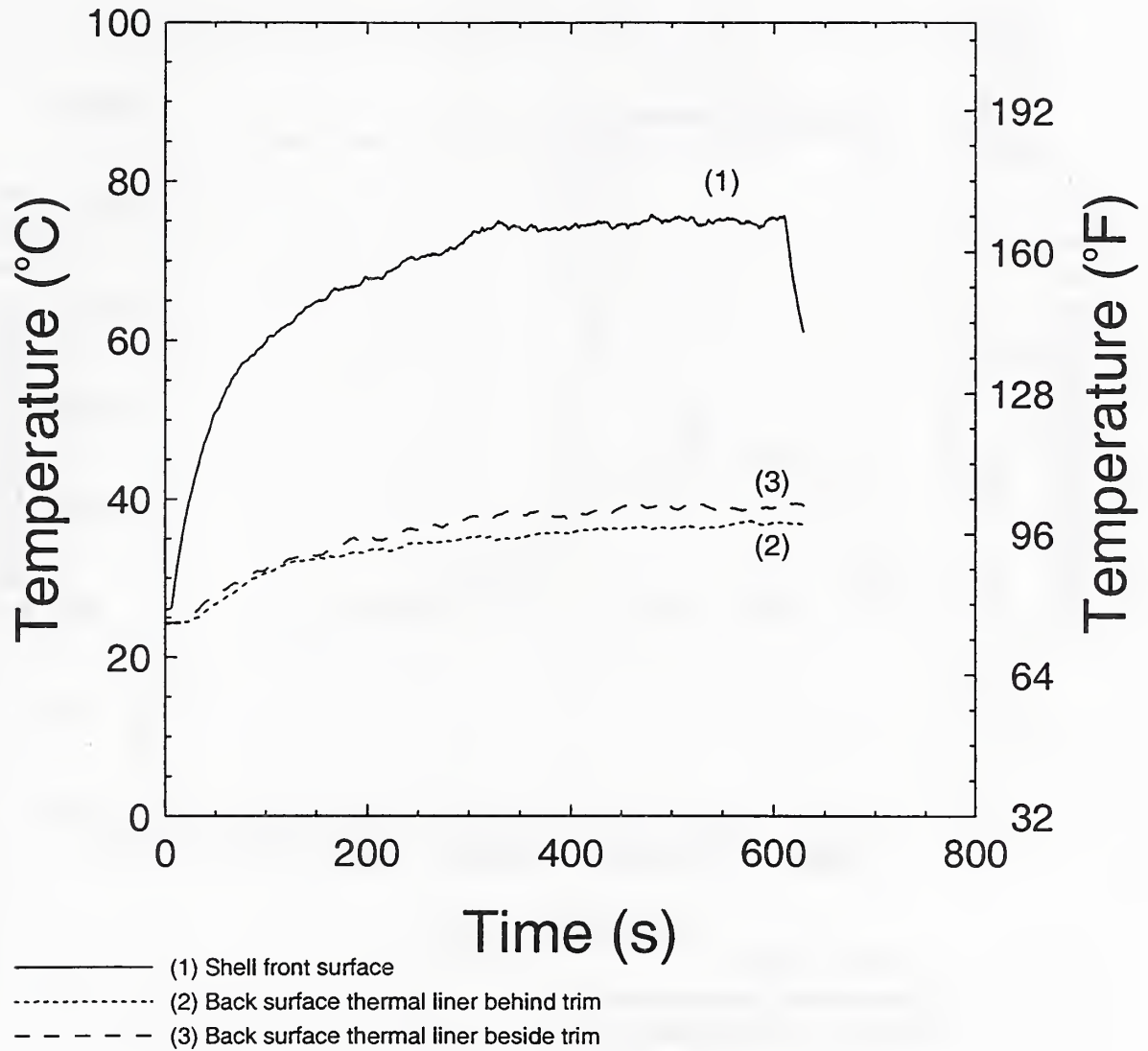


Figure 18 Data plots from 1.0 kW/m² heat flux test.

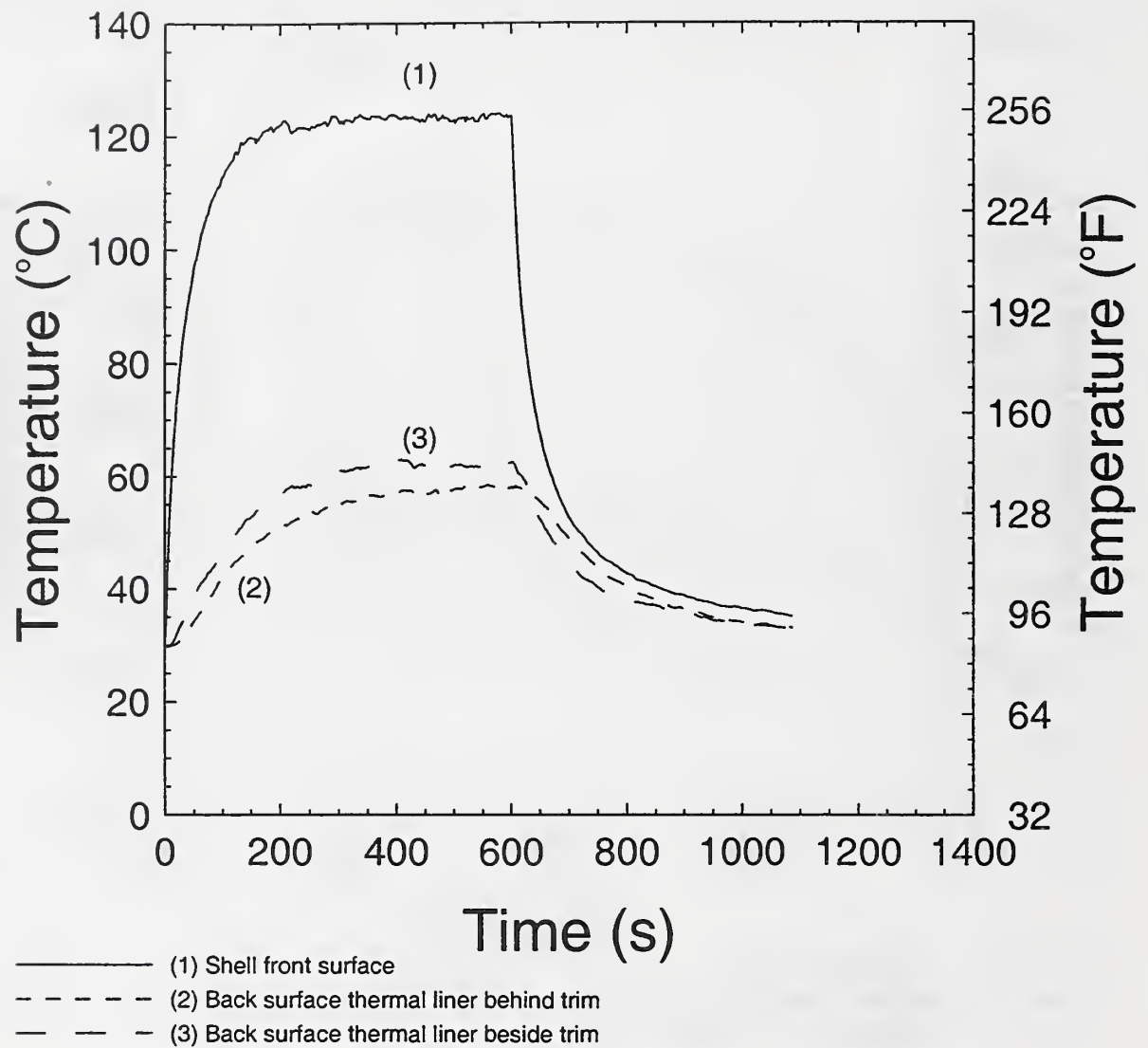


Figure 19 Data plots from 2.5 kW/m² heat flux test with dry thermal liner.

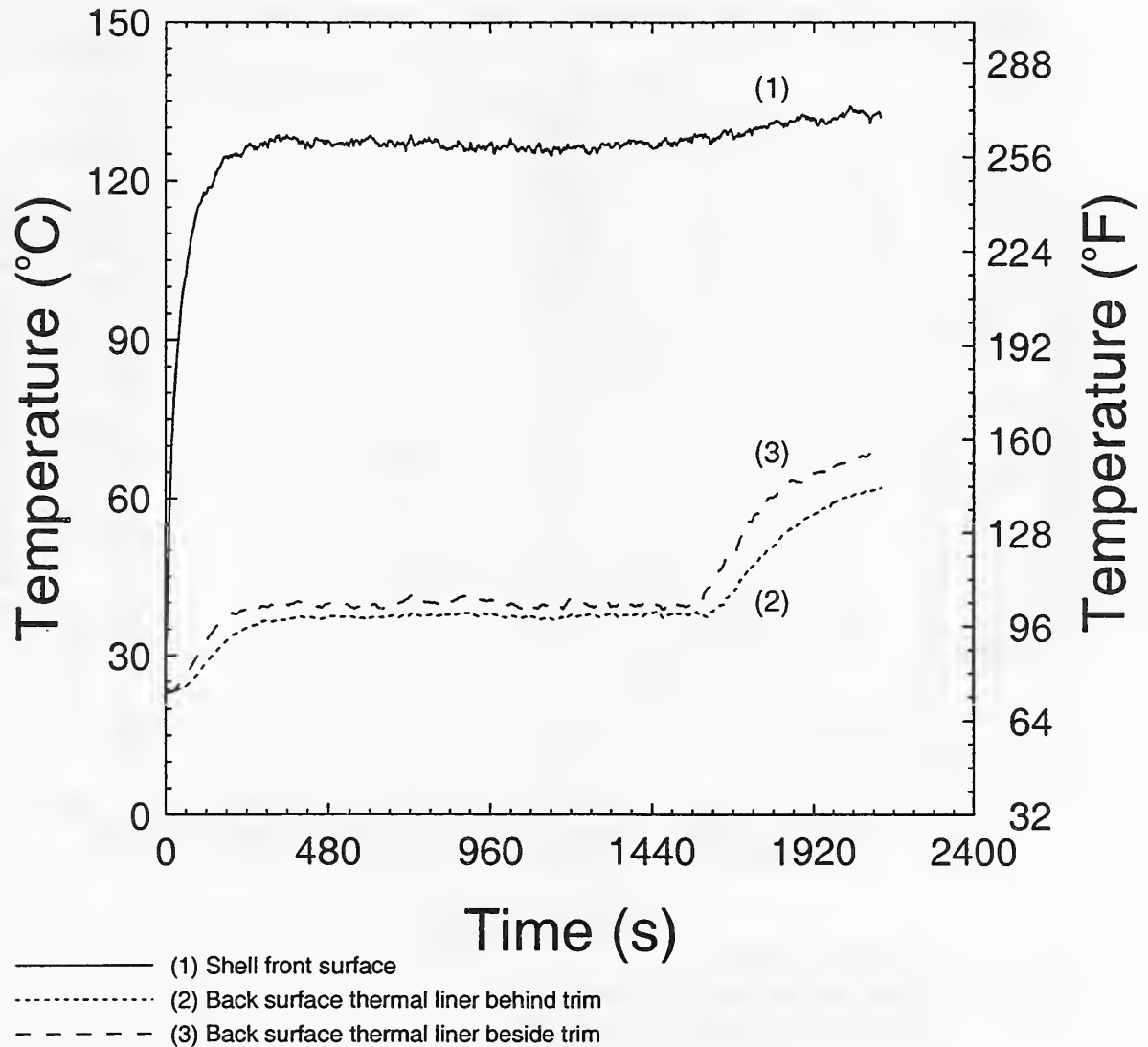


Figure 20 Data plots from 2.5 kW/m² heat flux test with 38 grams of water on thermal liner.

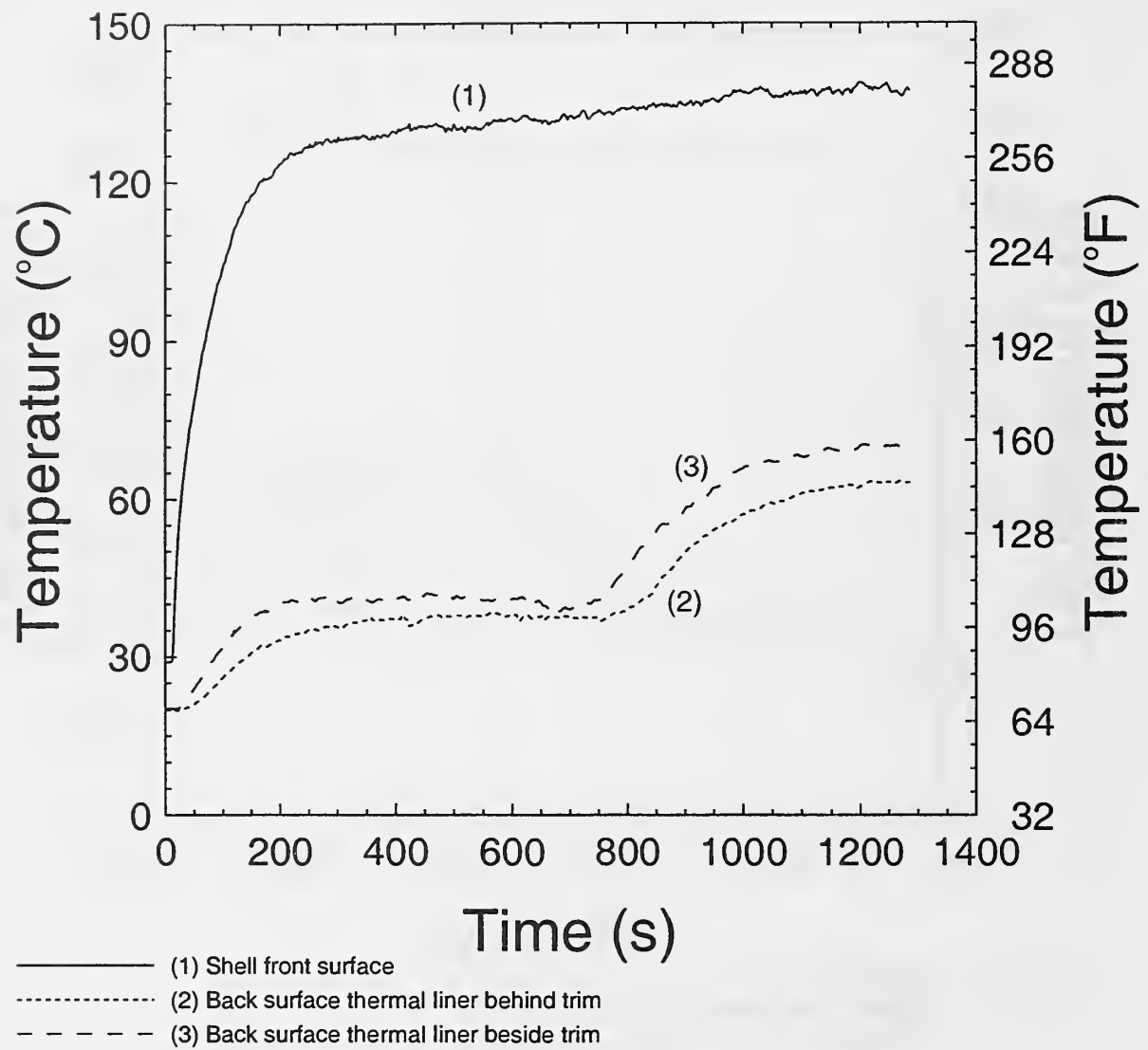


Figure 21 Data plots from 2.5 kW/m^2 heat flux test with 25 grams of water on thermal liner.

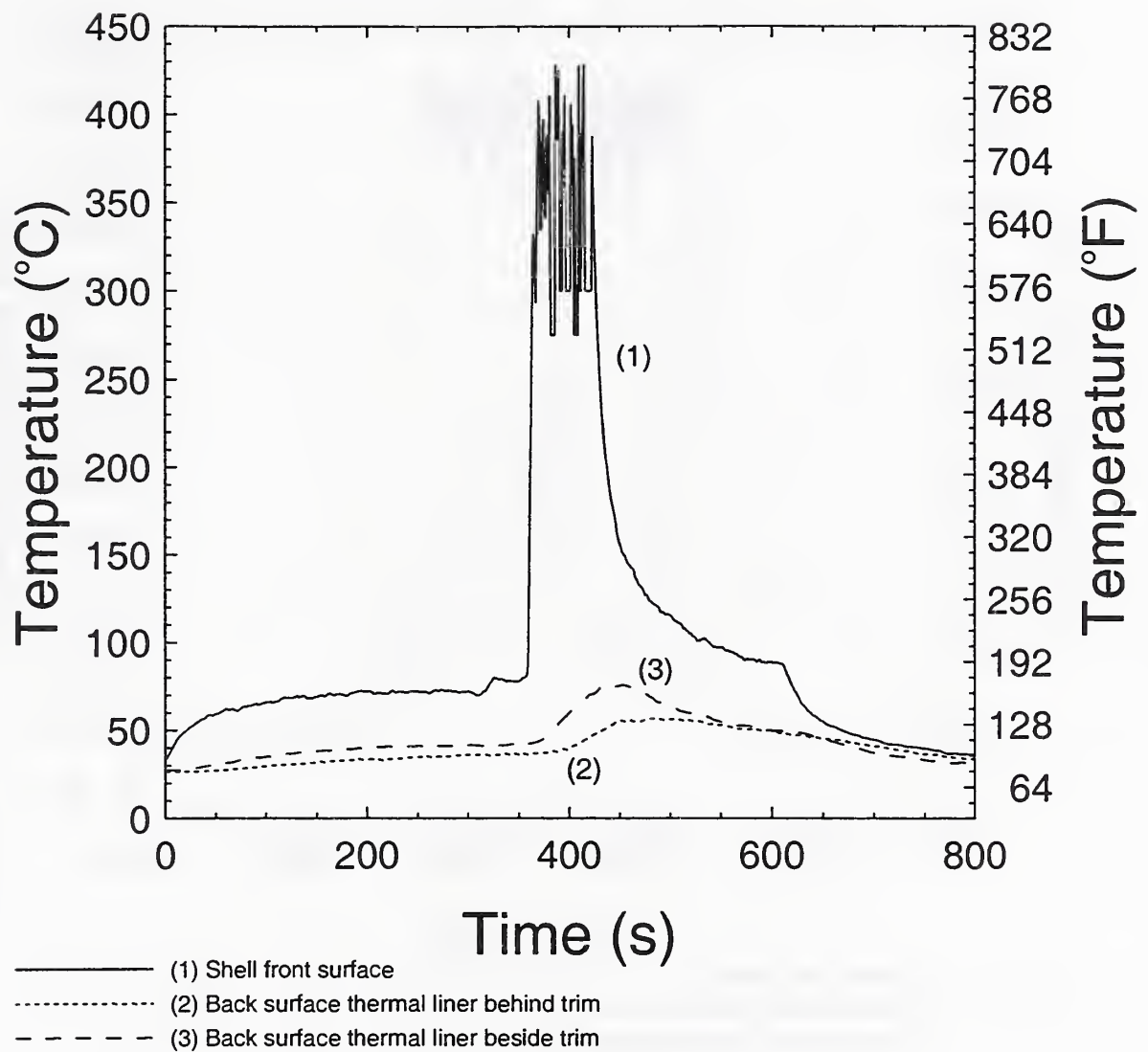


Figure 22 Data plots from dry specimen test, 1.0 kW/m^2 radiant plus flame $\sim 35 \text{ kW/m}^2$ total.

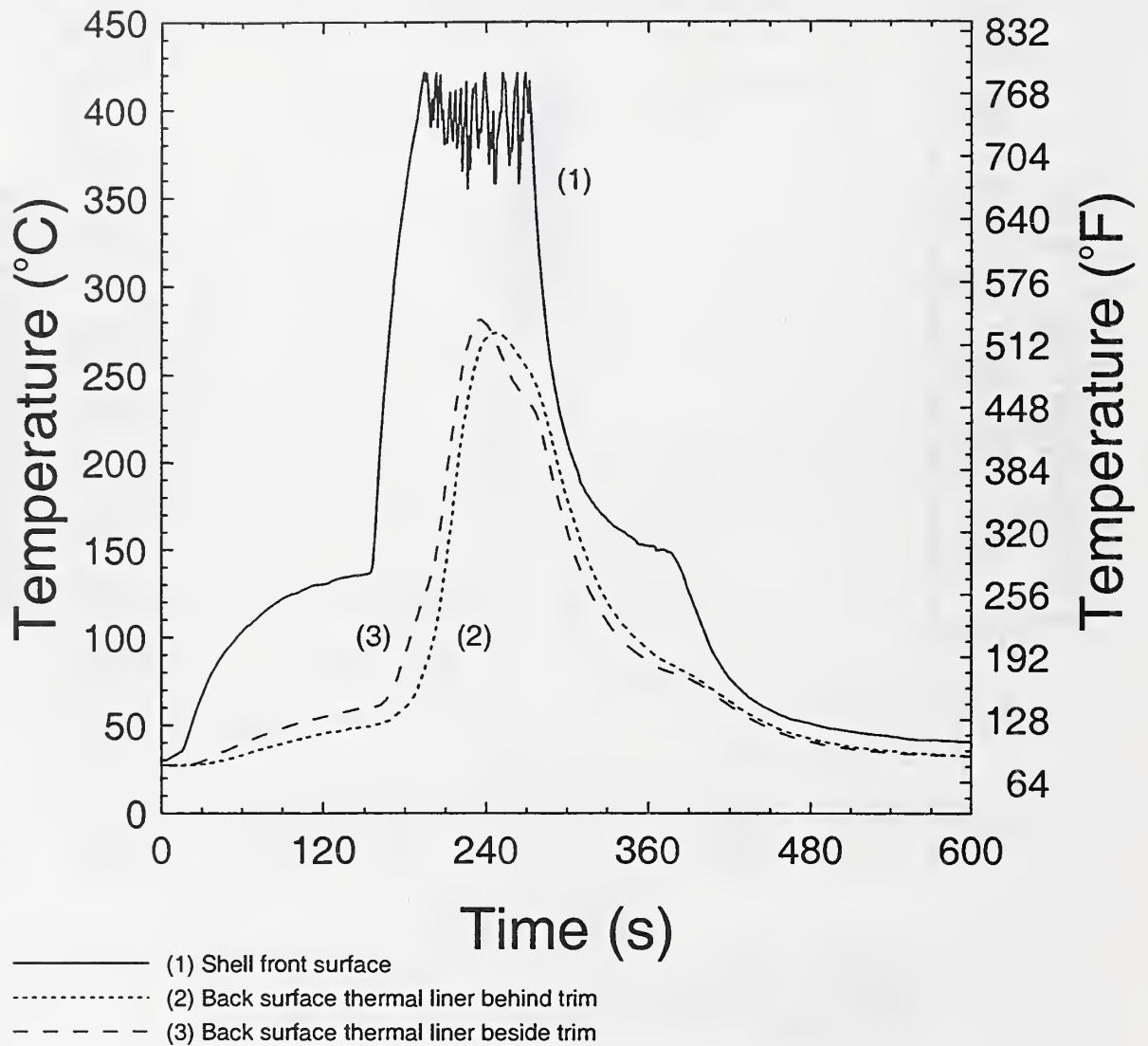


Figure 23a Data plots from 2.5 kW/m^2 , 20 kW/m^2 , plus flame test, dry specimen, top thermocouple set.

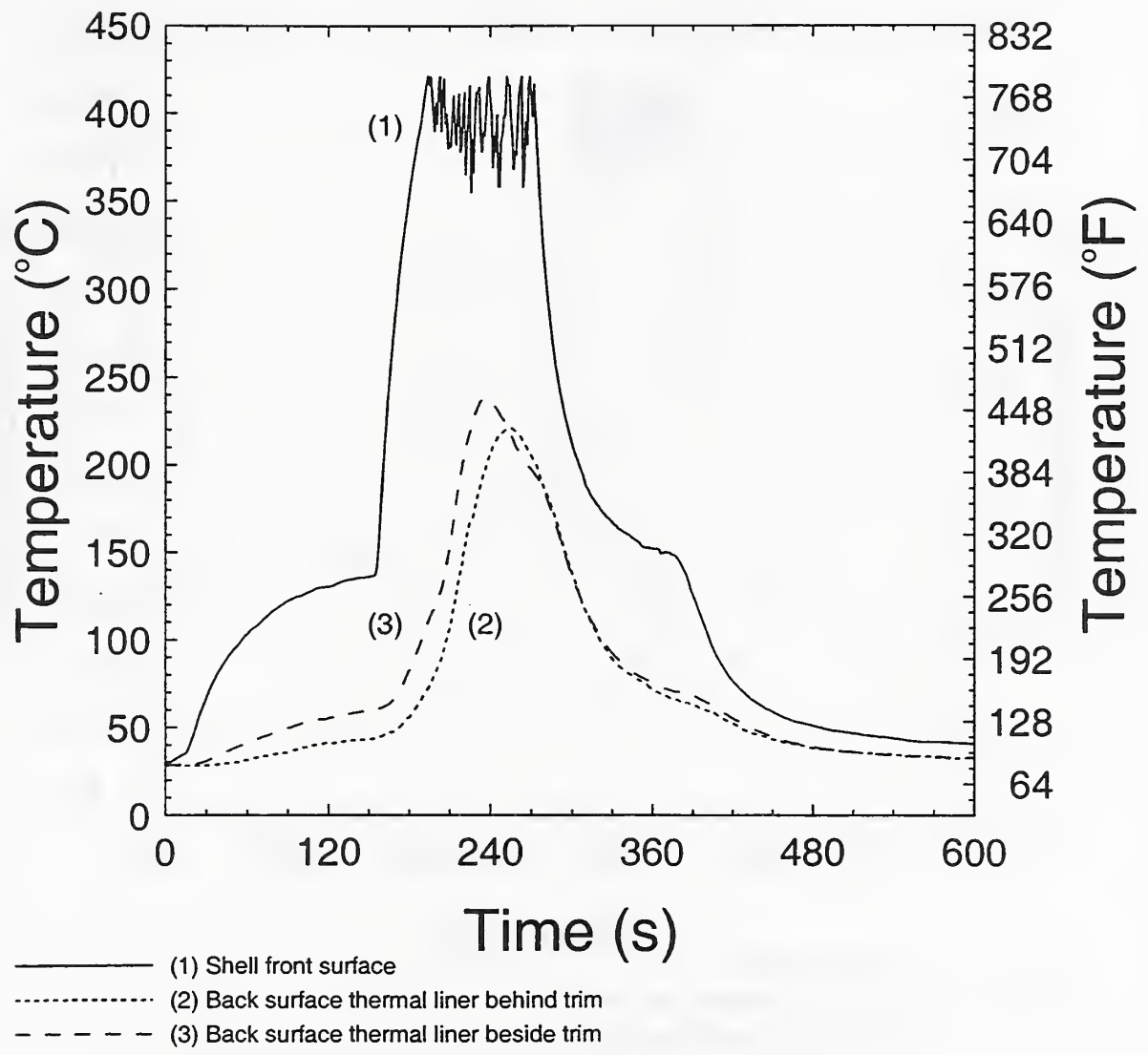


Figure 23b Data plots from 2.5 kW/m^2 , 20 kW/m^2 , plus flame test, dry specimen, center thermocouple set.

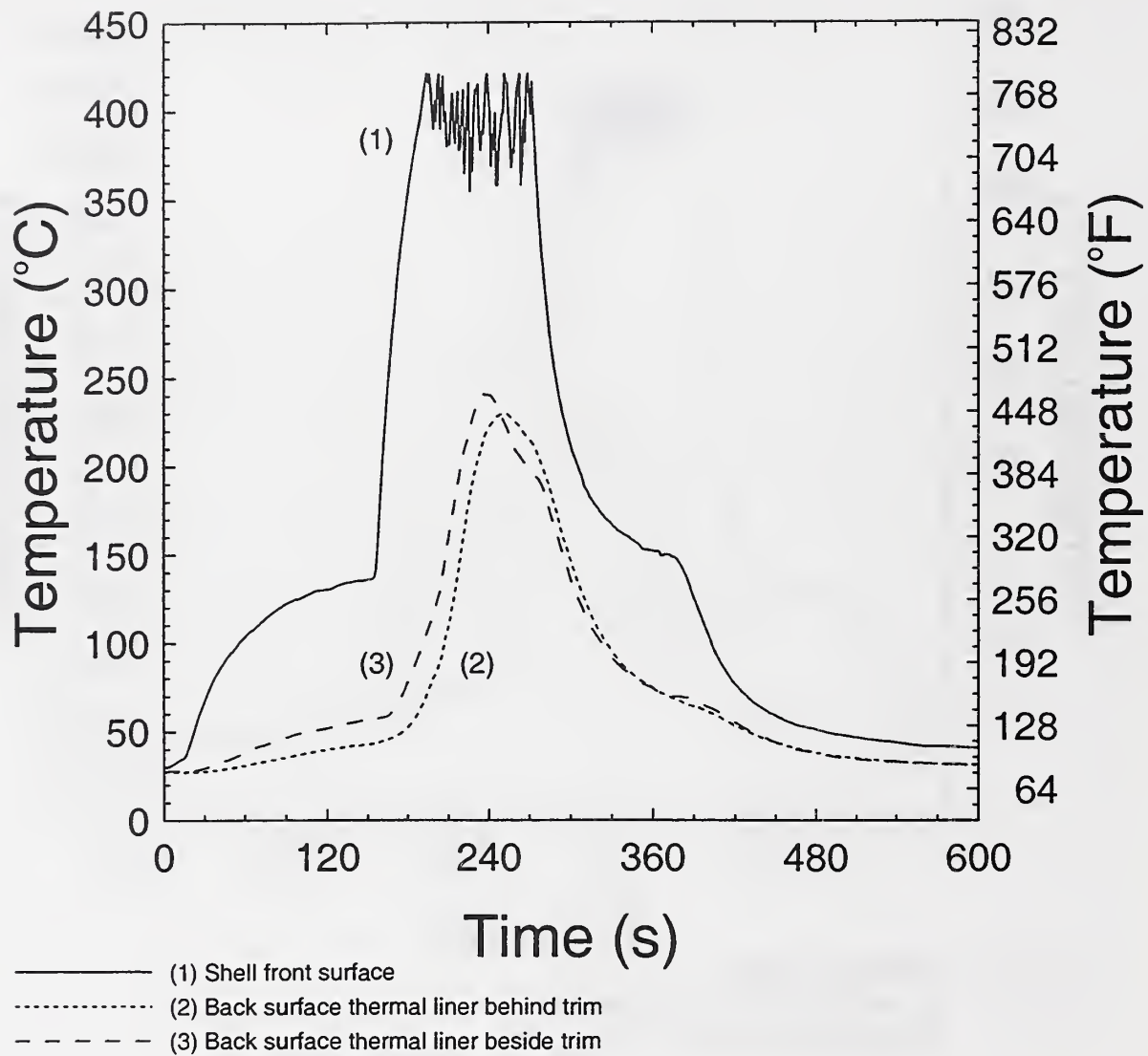


Figure 23c Data plots from 2.5 kW/m^2 , 20 kW/m^2 , plus flame test, dry specimen, bottom thermocouple set.

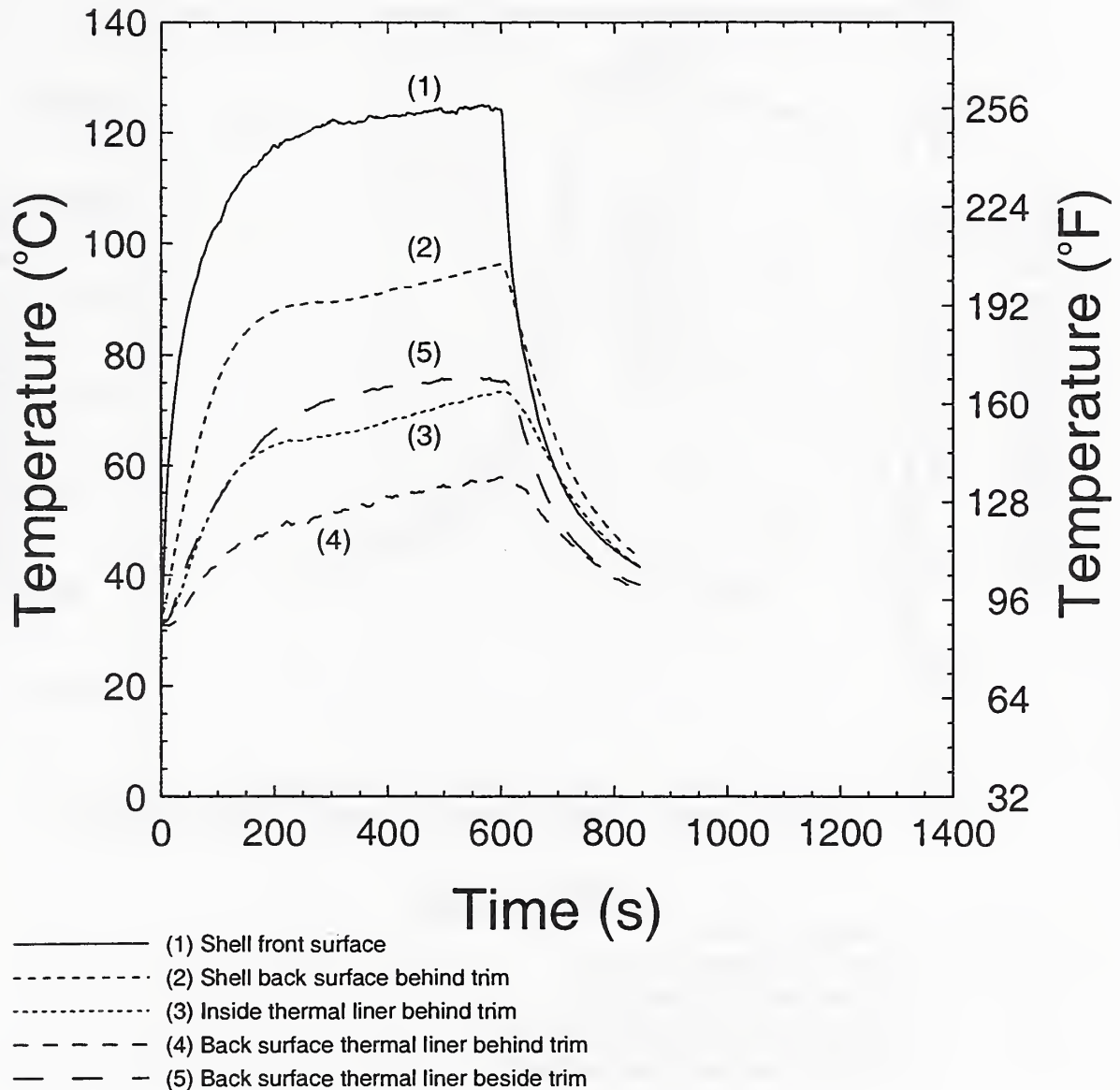


Figure 24 Data plots for a dry, open back, nonbreathable specimen at 2.5 kW/m^2 .

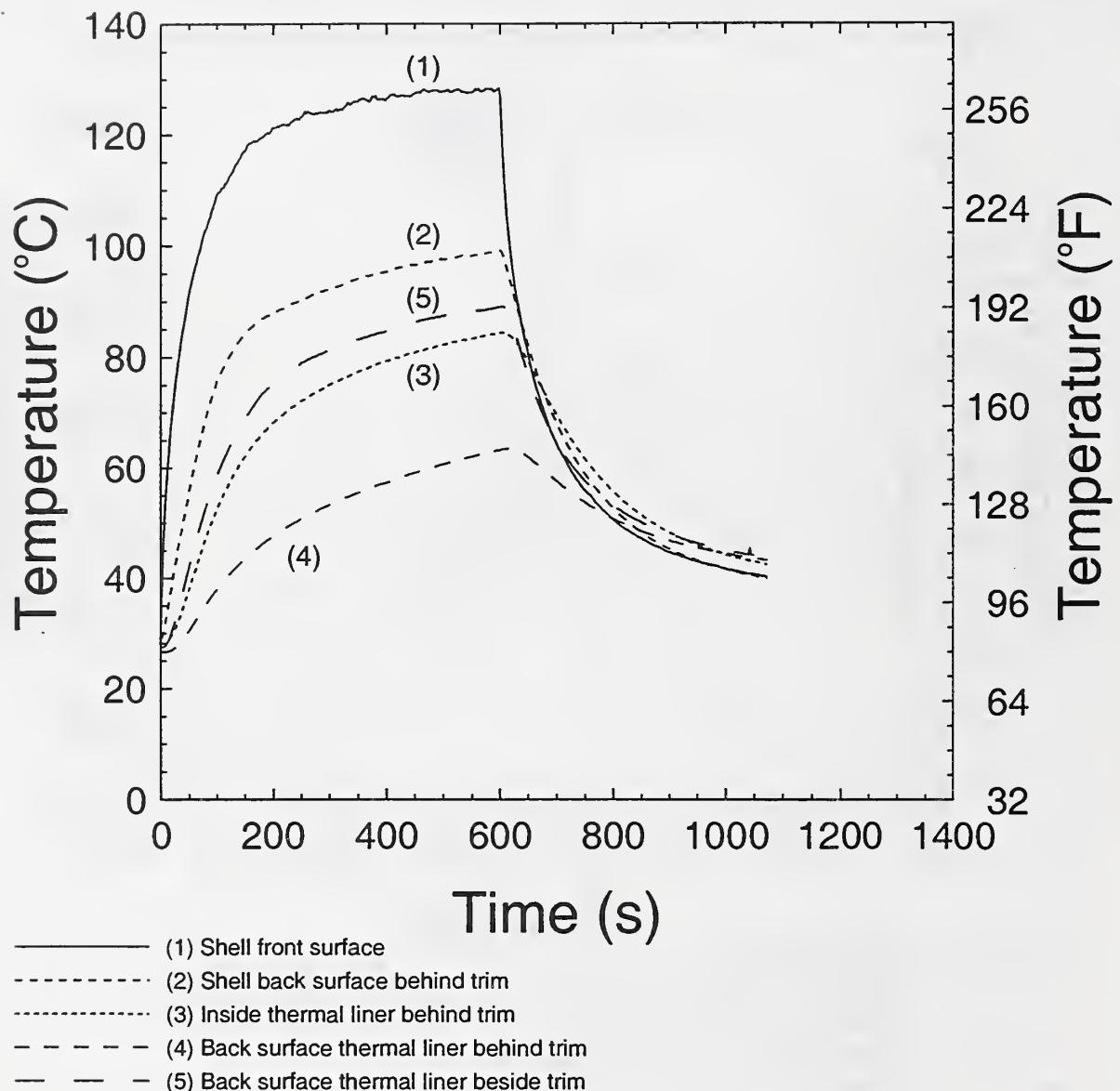


Figure 25 Data plots for a dry, closed back, nonbreathable specimen at 2.5 kW/m^2 .

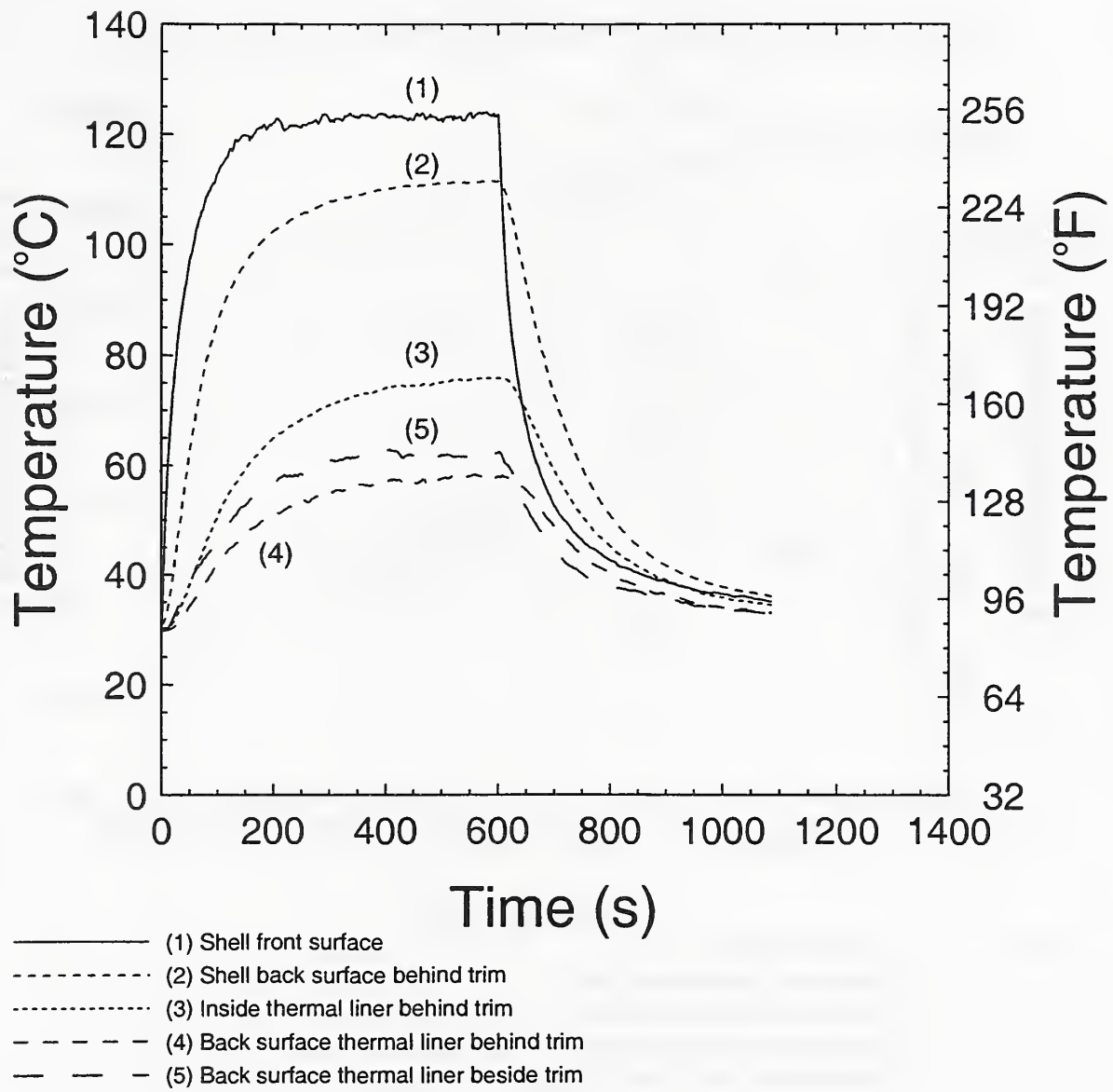


Figure 26 Data plots for a dry, open back, breathable specimen at 2.5 kW/m^2 .

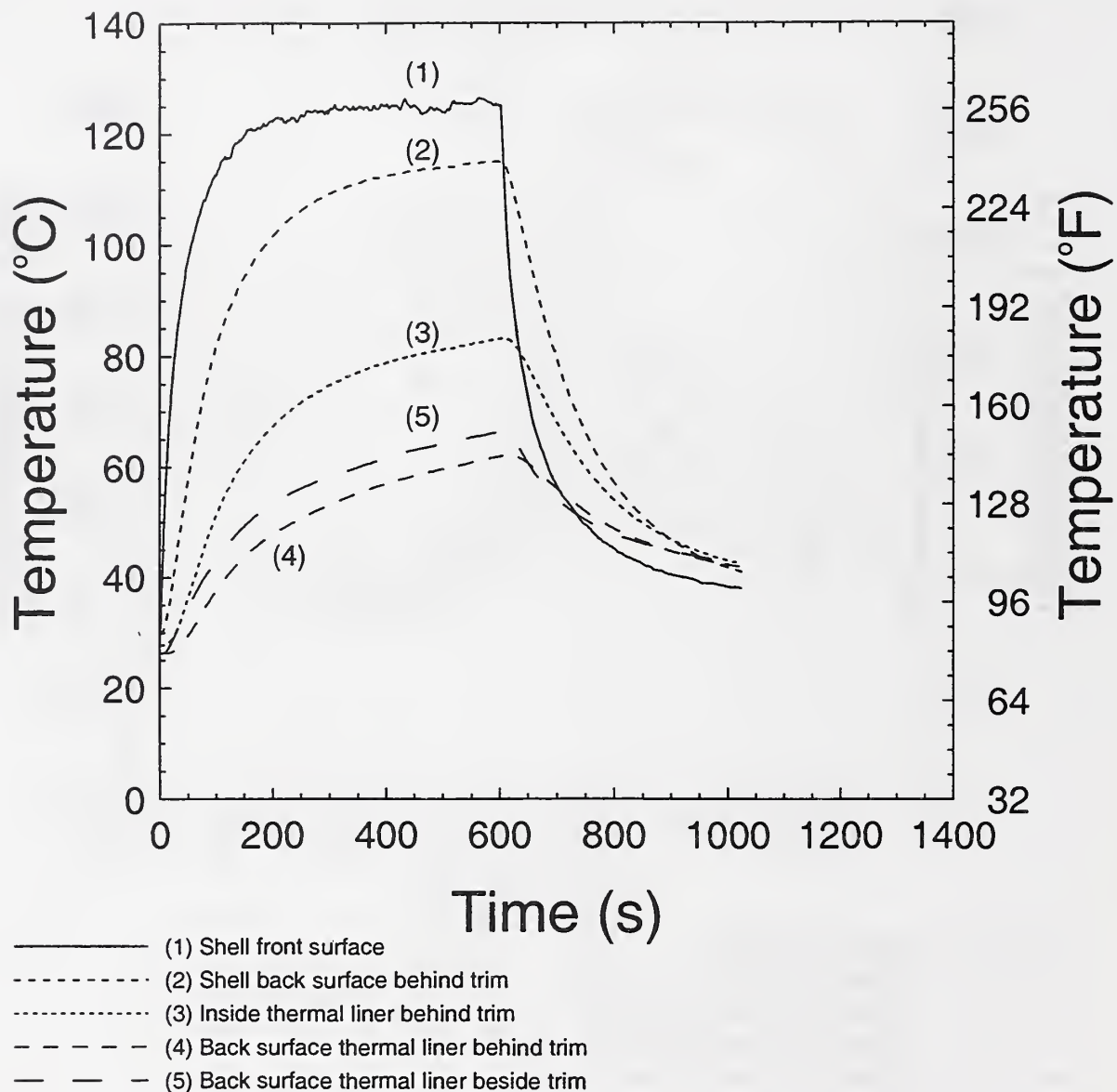


Figure 27 Data plots for a dry, closed back, breathable specimen at 2.5 kW/m^2 .

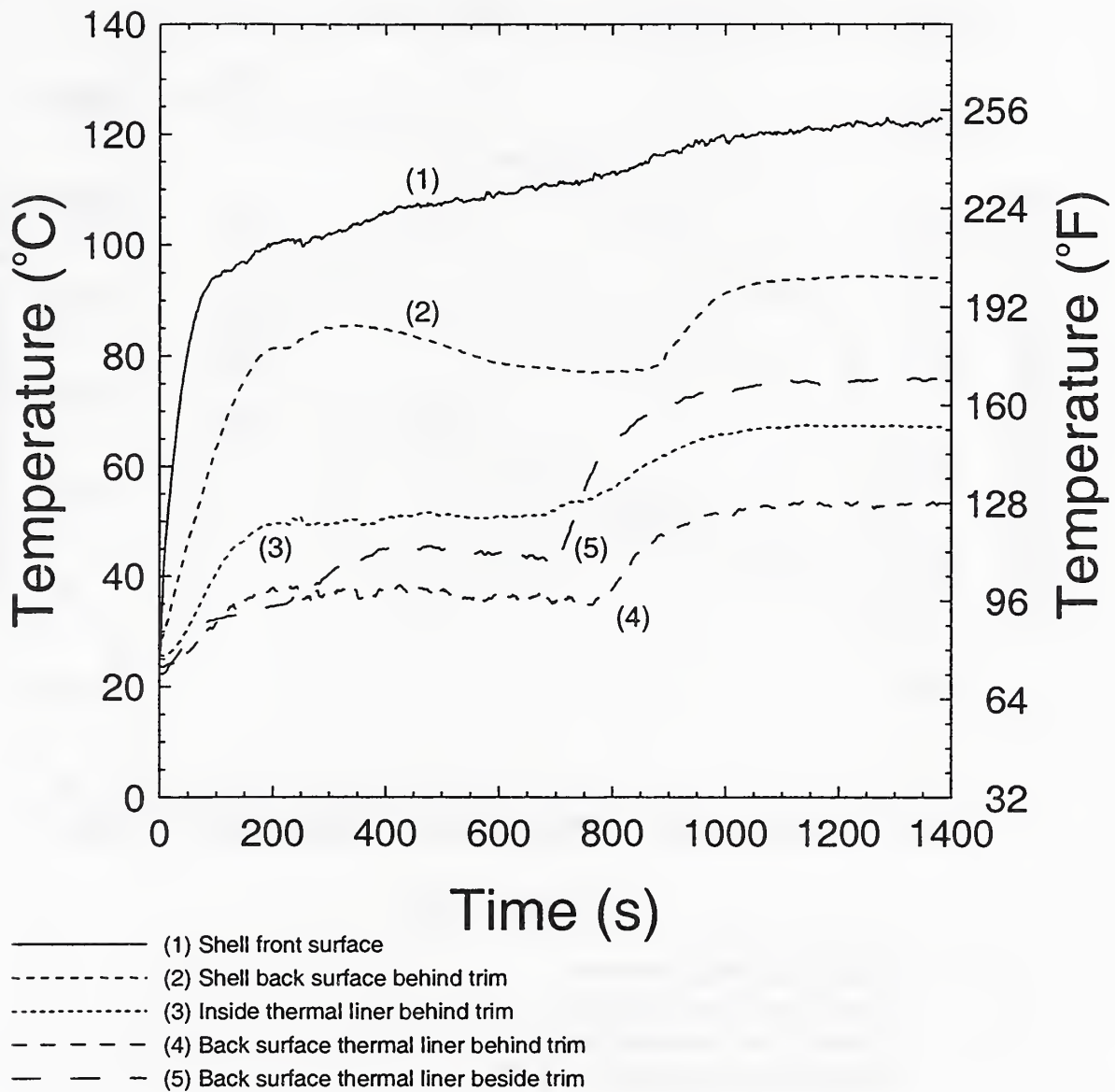


Figure 28 Data plots for wet, open back, nonbreathable specimen at 2.5 kW/m^2 .

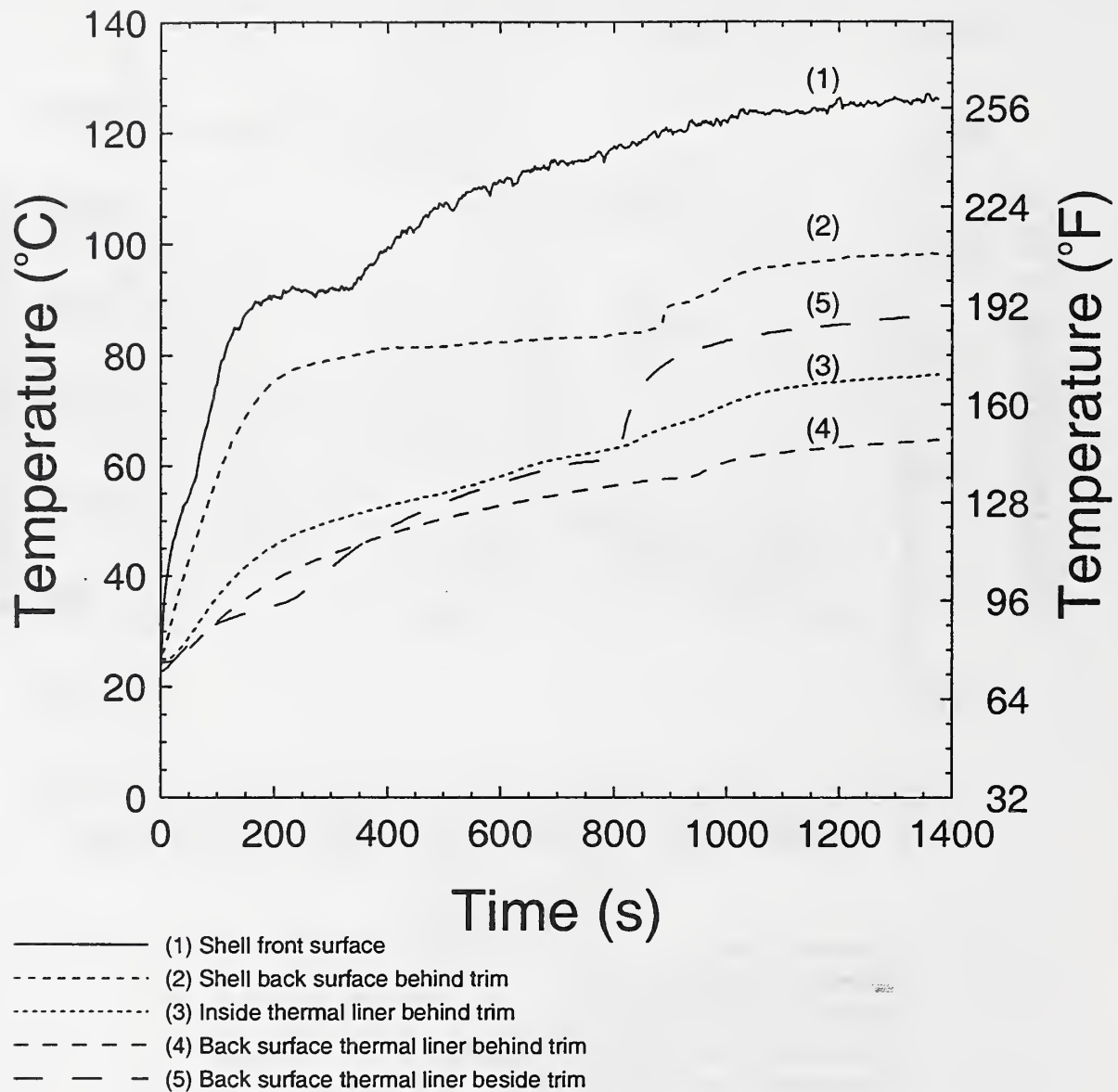


Figure 29 Data plots for a wet, closed back, nonbreathable specimen at 2.5 kW/m^2 .

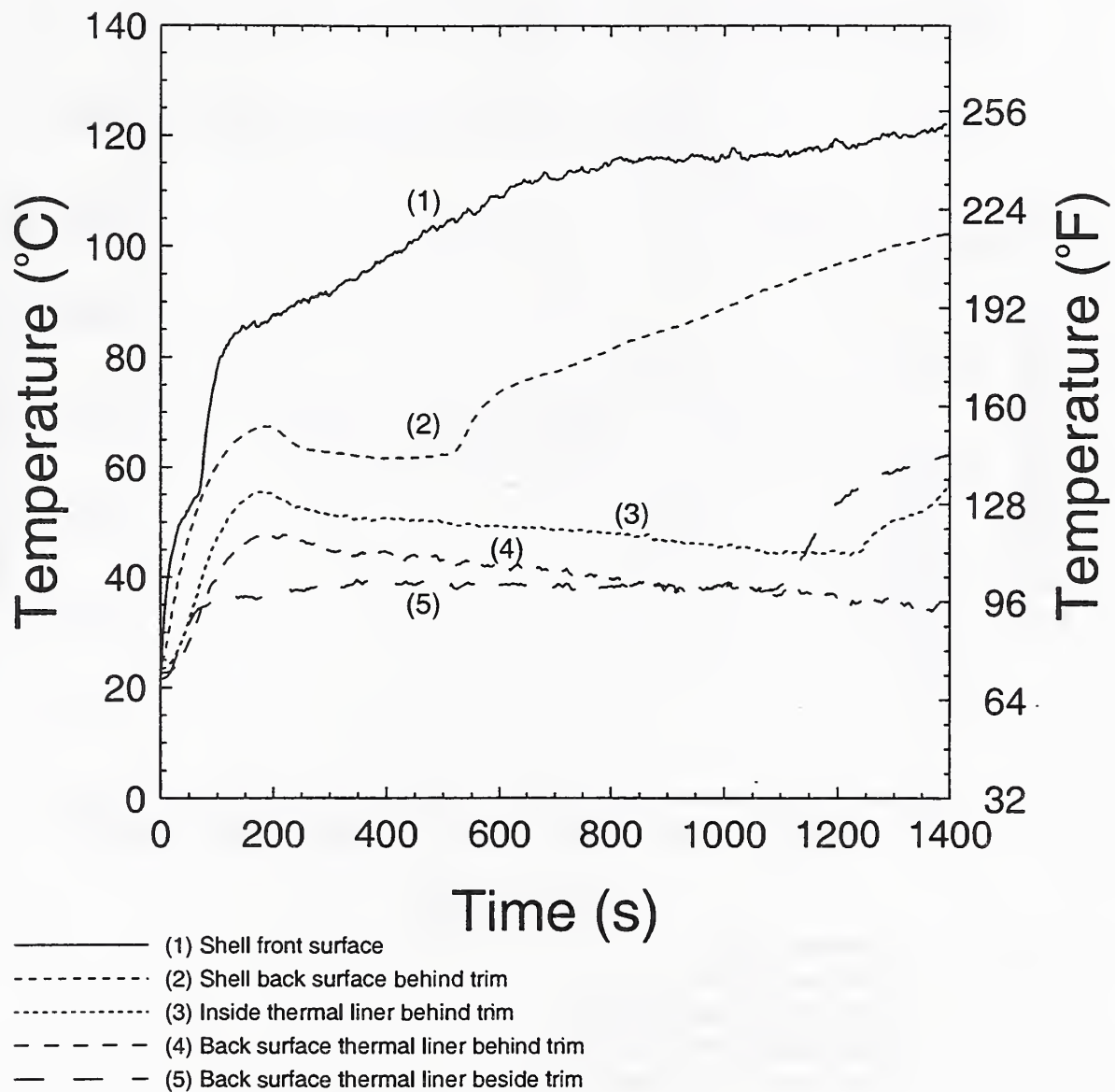


Figure 30 Data plots for a wet, open back, breathable specimen at 2.5 kW/m^2 .

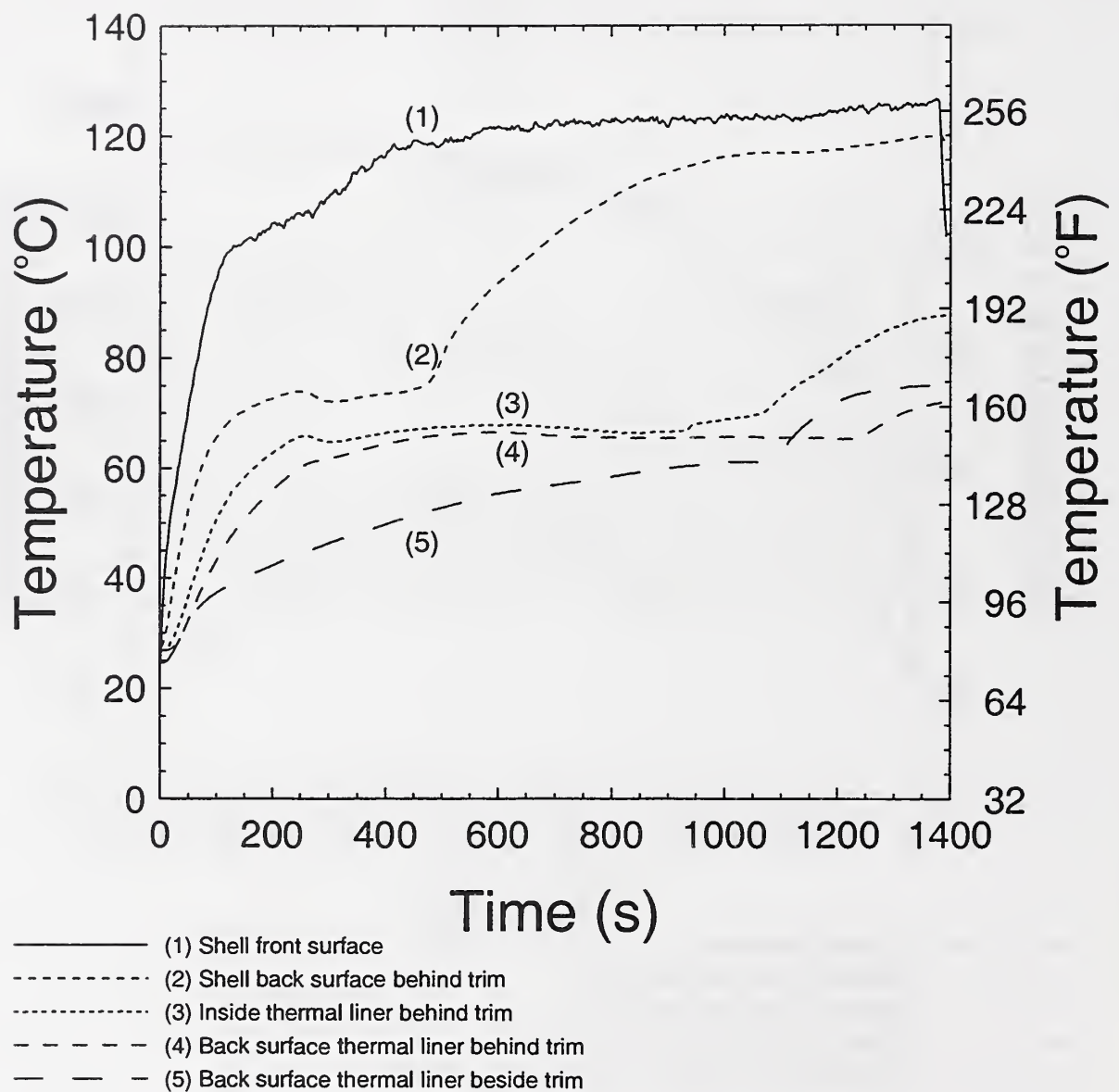


Figure 31 Data plots for a wet, closed back, breathable specimen at 2.5 kW/m^2 .

